Lakehead University

Speciation of Aqueous Hypercoordinated Organosilicate Complexes

By

Jiali Wen

A Thesis

Submitted to the Faculty of Graduate Studies

In Partial Fulfilment of the Requirements for the

Degree of Master of Science

Department of Chemistry

Thunder Bay, Ontario

December 2006

Library and
Archives Canada

Bibliothèque et
Archives Canada

Published Heritage
Branch

Direction du
Patrimoine de l'édition

395 Wellington Street
Ottawa ON K1A 0N4
Canada

395, rue Wellington
Ottawa ON K1A 0N4
Canada

NOTICE:
The author has granted a non-exclusive license allowing Library and Archives Canada to reproduce, publish, archive, preserve, conserve, communicate to the public by telecommunication or on the Internet, loan, distribute and sell theses worldwide, for commercial or non-commercial purposes, in microform, paper, electronic and/or any other formats.

AVIS:
L'auteur a accordé une licence non exclusive permettant à la Bibliothèque et Archives Canada de reproduire, publier, archiver, sauvegarder, conserver, transmettre au public par télécommunication ou par l'Internet, prêter, distribuer et vendre des thèses partout dans le monde, à des fins commerciales ou autres, sur support microforme, papier, électronique et/ou autres formats.

The author retains copyright ownership and moral rights in this thesis. Neither the thesis nor substantial extracts from it may be printed or otherwise reproduced without the author's permission.

L'auteur conserve la propriété du droit d'auteur et des droits moraux qui protège cette thèse. Ni la thèse ni des extraits substantiels de celle-ci ne doivent être imprimés ou autrement reproduits sans son autorisation.

In compliance with the Canadian Privacy Act some supporting forms may have been removed from this thesis.

Conformément à la loi canadienne sur la protection de la vie privée, quelques formulaires secondaires ont été enlevés de cette thèse.

While these forms may be included in the document page count, their removal does not represent any loss of content from the thesis.

Bien que ces formulaires aient inclus dans la pagination, il n'y aura aucun contenu manquant.

Canada

To my family

Abstract

Aqueous silicon chemistry plays a major and as yet unappreciated role in many fields of science. Emerging technologies such as the fabrication of biomimetic ceramics require a thorough understanding of all factors affecting aqueous silicon chemistry. In biology, silicon is known to be essential for the normal growth and development of most plants and animals, and yet almost nothing is known of the chemical mechanisms by which it is absorbed, transported and ultimately used. A careful characterization of silicon's interaction with sugars and sugar derivatives would be a significant step forward to unraveling this element's enigmatic biological role. In this study, ^{29}Si and ^{13}C NMR spectroscopy were employed to determine the structures and stability constants of aqueous silicon complexes formed with organic ligands containing either proximal hydroxy or vicinal *cis*-diol functionality.

Five-coordinated Si complexes formed with acyclic polyhydroxy molecules (polyols) are structurally analogous to the monomeric [(L=)$_2$SiOH]$^-$ species obtained with furanoidic *cis*-diol molecules, each with a single silicon centre bound via ester linkages to two bidentate ligands. Polyol complexes tend to be shorter lived, however, owing to ligand-ligand steric interactions. Glucoheptonic acid has a unique polyol configuration which enables it to wrap around a silicon centre with all of its hydroxyl groups directed inwards, yielding long-lived *mono*-ligand complexes that contain two ([L=Si(OH)$_3$]$^-$), three ([L≡Si(OH)$_2$]$^-$) or four ([L≡SiOH]$^-$) ester linkages (in addition to the usual array of labile *bis*-ligand complexes).

i

Two distinct hexaoxosilicon *tris*-ligand structures occur in highly alkaline

solutions containing either acyclic polyol or furanoidic *cis*-diol ligands. They are

inequivalent diastereomers of $[(L=)_3Si]^{-2}$, with delta-delta-delta and delta-delta-lambda

ligand configurations. If the ligands are very bulky, as in the case of the

ribonucleosides guanosine and adenosine, the delta-delta-lambda diastereomer is

nearly absent owing to severe ligand-ligand steric interference. It was therefore

surprising to discover that solutions containing certain mixtures of ribonucleosides

(adenosine and guanosine, adenosine and uridine, guanosine and cytidine), contain

both the delta-delta-delta and delta-delta-lambda diastereomers. The latter

configuration brings the different ribonucleoside base groups face to face, inferring

that the delta-delta-lambda diastereomer in mixed-ligand systems is stabilized by

multi-point H-bonding or π-stacking interactions between the bases.

The ligand binding affinities of silicon and boron were compared for

representative polyols (D-arabitol and D-gluconic acid) and furanoidic *cis*-diols (*cis*-

1,2-cyclopentanediol, 1,4-anhydroerythritol, guanosine). The stability constants of the

boron *bis*-ligand complexes at 24 °C did not vary significantly between the different

ligands (205 ± 10 for polyols, 69 ± 23 for vicinal *cis*-diols). These values were

roughly two orders of magnitude higher than those obtained for the analogous *bis*-

ligand silicon complexes. Gluconic acid and guanosine exhibited relatively large Si

binding affinities, however, for both *bis*-ligand (K = 10.8 and 1.3, respectively) and

tris-ligand (K = 175 and 13, respectively) complexes. These results indicate that silicon

might play a similar mechanistic role as boron in biological systems in which the

dissolved Si concentration generally far exceeds that of B.

Acknowledgments

I would like to express my gratitude to Dr. Stephen D. Kinrade for his role as my supervisor. I truly appreciate all of his extensive knowledge, support and advice during my graduate project. I learned many invaluable lessons from him. I also wish to thank Dr. Craig MacKinnon and Dr. Robert Mawhinney for their expert advice.

Additional thanks go to: the members of the Prairie Regional NMR Facility (Winnipeg) and Dr. Christopher T. G. Knight for obtaining the ^{29}Si NMR-600MHz and 750 MHz data; Ainsley Bharath and Debbie Leach in the Department of Chemistry for their assistance with supplies and materials; and Keith Pringnitz and Al Mackenzie in the Lakehead University Instrumentation Laboratory for NMR and SEM training.

I would also thank all the past members of the Kinrade research group with whom I have had the pleasure of working.

Finally, I like to take this chance to thank my husband, my parents and my two sons for all of their love, especially my mother who gave full support to my studies. I have had so much wonderful time and fun during my research project with my family's understanding and encouragement. Thank you all!

Contents

List of Tables

List of Figures

enrichment), 1.16 mol kg^{-1} NaOH and 2.1 mol kg^{-1} sodium

glucoheptonate.

2.48 mol kg^{-1} D-arabitol and 1.06 mol kg^{-1} Na$^+$; (b$_1$) 0.89 mol kg^{-1}

SiO$_2$, 2.23 mol kg^{-1} potassium D-gluconate and 2.67 mol kg^{-1} Na$^+$;

and (b$_2$) 1.02 mol kg^{-1} SiO$_2$, 2.32 mol kg^{-1} potassium D-gluconate

and 1.02 mol kg^{-1} Na$^+$.

Na^+; (b_1) 0.96 mol kg^{-1} SiO_2, 2.66 mol kg^{-1} anhydroerythritol and

3.00 mol kg^{-1} Na^+; and (b_2) 0.96 mol kg^{-1} SiO_2, 2.45 mol kg^{-1}

anhydroerythritol and 1.00 mol kg^{-1} Na^+.

Figure 3.4.5.   Silicon-29 NMR (99.36 MHz) spectra of solution adjusted pH 12.00

± 0.01 containing: (a_1) 0.85 mol kg^{-1} SiO_2, 0.43 mol kg^{-1} guanosine

and 1.82 mol kg^{-1} Na^+ at 22 °C; (a_2) 0.85 mol kg^{-1} SiO_2, 0.43 mol

kg^{-1} guanosine and 1.82 mol kg^{-1} Na^+ at 2 °C; and (b) 0.43 mol kg^{-1}

SiO_2, 0.86 mol kg^{-1} guanosine and 1.72 mol kg^{-1} Na^+ at −5 °C.

Figure 3.4.6.   Boron-11 NMR (160.33 MHz) spectra at 24 °C corresponding to

solutions that have been adjusted to pH 12.03 ± 0.03 and contain: (a)

0.10 mol kg^{-1} H_3BO_3; (b) 0.11 mol kg^{-1} H_3BO_3 and 0.11 mol kg^{-1}

D-arabitol; (c) 0.10 mol kg^{-1} H_3BO_3 and 0.10 mol kg^{-1} gluconic acid;

(d) 0.11 mol kg^{-1} H_3BO_3 and 0.11 mol kg^{-1} cis-1,2-cyclopentanediol;

(e) 0.10 mol kg^{-1} H_3BO_3 and 0.10 mol kg^{-1} 1,4-anhydroerythritol;

and (f) 0.11 mol kg^{-1} H_3BO_3 and 0.11 mol kg^{-1} guanosine.

Symbols and Abbreviation

Abbreviation

DDW   deionized distilled water (type I)

NOE   nuclear overhauser effect

FEP   fluorinated ethylene propylene

TFE   tetrafluoroethylene

LDPE   low density polyethylene

ICP-AES   inductively coupled plasma-atomic emission spectrometry

ICP-OES   inductive coupled plasma-optical emission spectrometry

NMR   nuclear magnetic resomance

SEM   scanning electron microscopy

EDS   energy dispersive spectroscopy

ppm   parts per million

Symbols

δ NMR chemical shift (ppm)

J nuclear spin-spin coupling constant

K equilibrium constant

Chapter 1 –Introduction

1.1   Importance of aqueous silicon

Aqueous silicon chemistry plays a major role in a number of important and topical fields [1-5]. The two most abundant elements of the Earth's crust, silicon (27.7%) and oxygen (46.6%), are the basic building blocks of silicates, the largest and most complex mineral group. Silicate minerals interact with water on a massive scale, yielding life-sustaining soils and mineral deposits along with dissolved silicon in the form of monomeric (H_4SiO_4) and various oligomeric silicate species. Aqueous silicates are used in industry for the production of a wide range of products ranging from adhesives to zeolite catalysts [6-7]. In the biological world, aqueous silicon is taken up and used by most organisms and, indeed, it is truly essential for the growth and development of numerous fungi, lichens, algae (diatoms) and primitive plants [8-11]. Higher plants such as bananas, tomatoes, sugarcane, grass, wheat and rice exhibit increased susceptibility to a wide range of biotic and abiotic stresses if they are deprived of silicon [12-17]. In animals, it is needed to maintain healthy growth of connective tissue including bone and cartilage [18-21]. Chicks fed silicon-deficient diets exhibit structural abnormalities in their skulls and long bones, poorly formed joints, plus defective growth of endochondral and articular cartilage [22-23]. Similar abnormalities have been observed in silicon-deprived rats [24-29]. Silicon deficiency in humans has been linked to heart disease, cancer, osteoporosis and neurodegenerative disorders [30-33]. The modern Western diet is low in silicon owing to food processing and water treatment practices. The most important dietary sources

1

are grain products (including beer), bananas and green beans [34-36]. Food

supplements may have promise for clinical treatment of diseases such as connective

tissue disorder and osteoporosis [37]. Remarkably, almost nothing is known at the

molecular level about the uptake, transport and biofunctionality of this important

element [38].

1.2 Aqueous silicon chemistry

In nature, silicon is usually found coordinated to four oxygens – although not

exclusively (see below). The notation system described by Kinrade *et al.* [39-40] is

used to denote the coordination number and the connectivity at silicate Si centres. $\underline{Q}$,

$\underline{P}$ and $\underline{H}$ are used to represent tetra-, penta- and hexaoxosilicon centres, respectively,

and a superscripted figure employed to indicate the corresponding number of siloxane

(Si-O-Si) linkages at each centre. For instance, the silicate monomer ($H_{4-q}SiO_4^{q-}$) is

represented by Q^0, the dimer ($H_{6-q}Si_2O_7^{q-}$) denoted by Q^1Q^1 or simply Q^1_2, and the

cyclic trimer ($H_{6-q}Si_3O_9^{q-}$) as $Q^1Q^1Q^1$ or simply Q^2_3. The subscripted figure indicates

the number of chemically equivalent centers in a symmetrical species.

The solubility of amorphous silica, SiO_2, is relatively low at pH 7, with

reported values ranging between 100 and 130 ppm at 25°C [41]. However, it

dramatically increases above pH 10. The main anion present under very dilute and/or

highly alkaline conditions is the silicate monomer. The equilibrium between the

different silicate anions is governed by the rules of polymer chemistry. The variety of

silicate anions in alkaline solutions rises as silicon concentration is increased, pH is

2

decreased and/or temperature is decreased. In solutions containing equimolar

concentrations of SiO_2 and alkali metal hydroxide there are as many as 42 different

silicate anions undergoing rapid chemical exchange with one another [42-47].

1.3   Acyclic polyol interactions with aqueous silicon

Kinrade and co-workers [40] have shown that stable, alkoxy-substituted

anions form when alcohols are added to highly alkaline silicate solutions. Moreover,

certain aliphatic polyhydroxy molecules ("polyols") such as mannitol, xylitol and

threitol were found to produce novel complexes containing either pentaoxo- or

hexaoxosilicon (Figure 1.1) [48]. These ligands all contain four or more adjacent

hydroxyl groups, with two being in *threo* configuration. The resulting complexes are

especially stable if there is also a carboxylate group on the ligand, existing even at pH

7 and biologically relevant silicon concentrations [49]. Hexacoordinated silicon

complexes tend to be favored over the pentaoxosilicon species under highly alkaline

conditions [39, 48, 50]. Molecular orbital modeling studies indicate that the silicon

diester bonding site on these polyol ligands is the *threo* pair of hydroxy groups [51-

53].

3
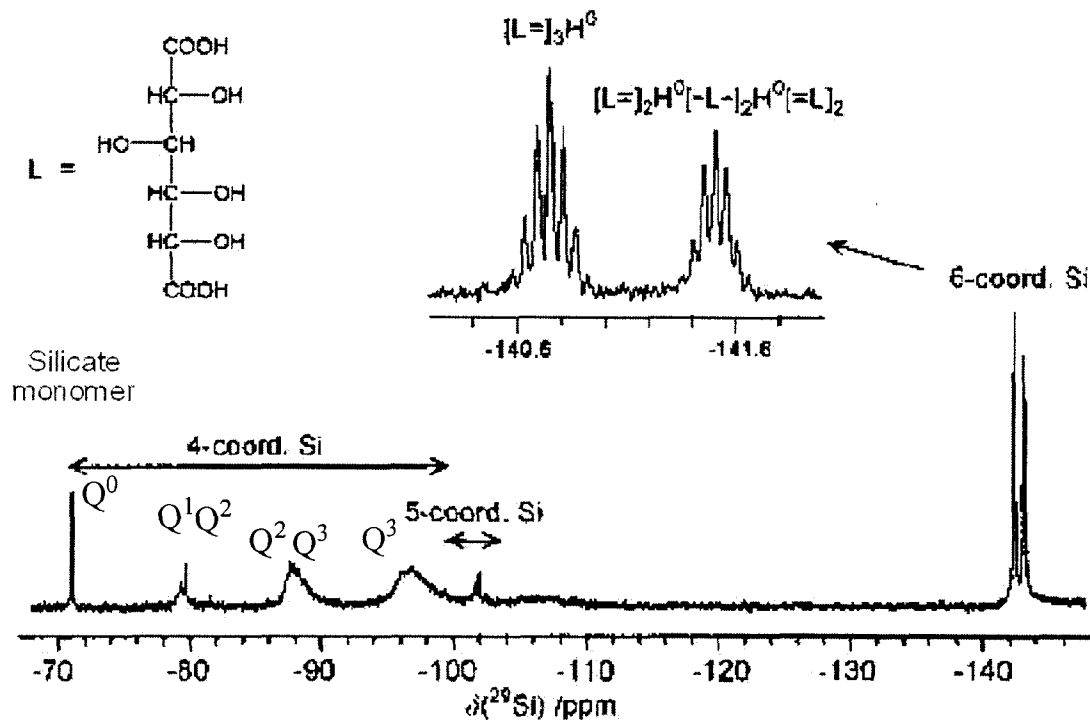
Figure 1.1. Silicon-29 NMR ^{1}H-coupled spectrum (99.36 MHz) of a solution containing 1.2 mol kg^{-1} SiO$_2$, 2.9 mol kg^{-1} NaOH and 1.7 mol kg^{-1} monopotassium D-saccharic acid at 298 K.

1.4 Furanoidic-1,2-*cis*-diol interactions with aqueous silicon

Furanoidic-1,2-*cis*-diol molecules are also capable of forming

hypercoordinated silicon complexes [54-56]. These include 1,4-anhydroerythritol,

cis-1,2-dihydroxycyclopentane, ribose along with various ribonucleosides (*e.g.*,

uridine, cytidine, guanosine) and ribonucleotides (ATP and NAD+) [54]. Silicon-29

NMR spectra of solutions containing pentaoxosilicon complexes are generally

4

characterized by three strong signals between *ca.* –97 and –102 ppm. Detailed

analysis has revealed that these resonances correspond to three different diastereomers

of the monomeric *bis*-(diolato)-hydroxo complex, [(L=)$_2$SiOH]⁻ (where L represents

the *cis*-diol ligand), in which the ligands are oriented in *syn-syn*, *anti-anti* or *syn-anti*

configuration [55-56].

1.5   Diester forming ability of boron and silicon compared

The biochemistry of boron is better understood than that of silicon. Boron,

like silicon, is able to form reversible diester bonds with molecules containing either

proximal hydroxy or vicinal *cis*-diol functionality in a favorable conformation [57-61].

Boron's coordination number in the resulting complexes is only 4, however. The

mechanistic basis for boron's biofunctionality appear to be related to this ability to

form reversible diester bonds with molecules such as rhamnogalacturonan-II (RG-II)

in plant cell walls [62], sorbitol in plant phloem extracts [63], bacterial signaling

molecule AI-2 [64], and a number of antibiotics [65]. Our objective here was to

compare silicon's binding affinity with that of boron in order to assess its potential for

taking part in the same kinds of biochemical processes.

5

Chapter2 – Experimental

2.1 General sample preparation

Type-I deionized/distilled water (DDW) was used throughout this study. It was purified through "macropure", "ultrapure" and "organic-free" resin cartridges (Barnstead E-pure) and then filtered (0.2μm). The silicon concentrations of the purified DDW and deuterated water (D_2O) used to provide a NMR field/frequency lock was below the ICP-AES (Varian Vista Pro Radial) detection limit of 0.02 μg L^{-1}. All samples were prepared and stored in containers of low density polyethylene (LDPE), Teflon FEP or Teflon TFE. Plastic labware was cleaned by successively soaking in 10% nitric acid, 10% hydrochloric acid, 0.01 M Na_2H_2EDTA and, finally, DDW. Solutions were transferred using non-lubricated polypropylene syringes (Sigma-Aldrich) in conjunction with Teflon FEP needles and LDPE pipettes.

The amorphous silica was prepared by hydrolysis of $SiCl_4$ at room temperature, followed by repeated rinsing with DDW until the pH value was equal to that of the DDW (*ca.* pH 5.7), and then dried at 110 °C for 24 hours.

Sodium hydroxide stock solutions were made by mixing NaOH pellets (99.998%) with pre-boiled DDW, and then titrated against potassium hydrogen phthalate using a 1% phenolphthalein indicator.

6

Sodium silicate solutions were prepared by tumbling aqueous NaOH with dried amorphous silica at 70 °C, or by heating ^{29}Si-enriched silica with aqueous NaOH for 24 hours at 220 °C in a PTFE-lined pressure vessel.
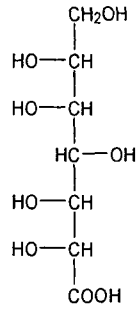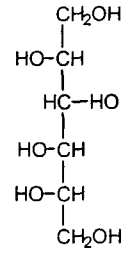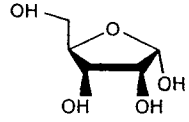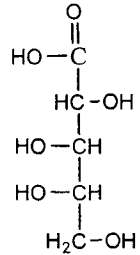
pH measurements were performed at room temperature or 0 °C using an Orion Ross combination semi-micro pH electrode, calibrated at pH 4.00, 7.00, and 10.00 prior to each use.
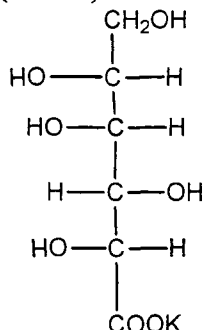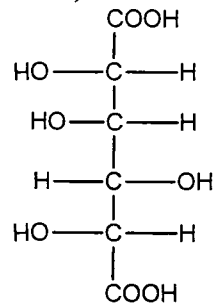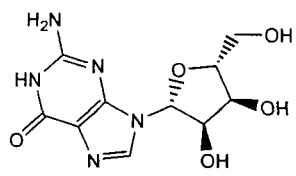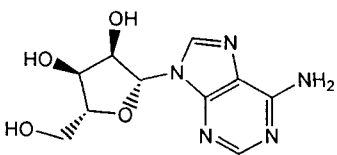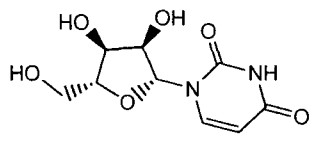
The chemical reagents employed in this study are listed in Table 2.1.
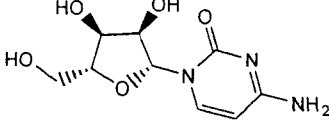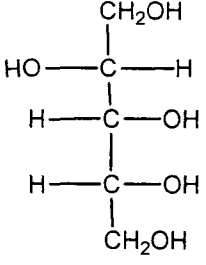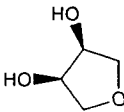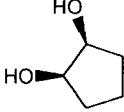
Table 2.1. Chemical reagents

Reagent	Supplier/Purity	Molecular formula/structures ($F.W.$ /g mol^{-1})	pKa
silicon tetrachloride	Sigma-Aldrich / 99.998 %	$SiCl_4$ (169.9)	9.21
deuterium oxide	Sigma-Aldrich / 99.9 atom% ^{2}H	^2H_2O (20.03)	5.5
sodium hydroxide	Sigma-Aldrich / 99.998 %	NaOH (40.00)	–
hydrochloric acid	Sigma-Aldrich / 37 %	HCl (36.46)	-4
silicon-29 oxide (amorphous)	Isonics / 99.35 atom% ^{29}Si	$^{29}SiO_2$ (60.97)	–

boric acid	Sigma-Aldrich / 99.998%	H_3BO_3 (61.83)	9.14, 12.74, 13.8
α-D-glucoheptonic acid, sodium salt	Sigma-Aldrich	$C_7H_{13}O_8$ (248.2) $$\begin{array}{c} CH_2OH \\ | \\ HO-CH \\ | \\ HO-CH \\ | \\ HC-OH \\ | \\ HO-CH \\ | \\ HO-CH \\ | \\ COOH \end{array}$$	3.3
D-sorbitol	Sigma-Aldrich / 97 %	$C_6H_{14}O_6$ (182.17) $$\begin{array}{c} CH_2OH \\ | \\ HO-CH \\ | \\ HC-HO \\ | \\ HO-CH \\ | \\ HO-CH \\ | \\ CH_2OH \end{array}$$	–
D-ribose	Sigma-Aldrich / 98 %	$C_5H_{10}O_5$ (150.13)	–
D-fructose	Sigma-Aldrich / 99+ %	$C_6H_{12}O_6$ (180.16) $$\begin{array}{c} O \\ \| \\ HO-C \\ | \\ HC-OH \\ | \\ HO-CH \\ | \\ HO-CH \\ | \\ H_2C-OH \end{array}$$	–

8

potassium D-gluconate	Sigma-Aldrich / 99 %	$HOCH_2[CH(OH)]_4CO_2K$ (234.25)	–
D-saccharic acid monopotassium salt	Sigma-Aldrich / 98 %	$C_6O_8H_9K$ (248.24)	–
guanosine hydrate	Sigma-Aldrich / 98 %	$C_{10}O_5H_{11}N_5$ (283.24)	–
(-) adenosine	Sigma-Aldrich / 99+ %	$C_{10}O_4H_{11}N_6$ (267.25)	–
uridine	Sigma-Aldrich / 99 %	$C_9O_6H_{12}N_2$ (244.20)	–

cytidine	Sigma-Aldrich / 99 %	$C_9O_5H_{13}N_3$ (243.22)	–
D-arabitol	Sigma-Aldrich / 99 %	$C_5O_5H_{12}$ (152.15)	–
1,4-anhydroerythritol	Sigma-Aldrich / 95 %	$C_4O_3H_8$ (104.11)	–
cis-1,2-cyclopentanediol	Sigma-Aldrich / 98 %	$C_5O_2H_{10}$ (102.13)	–

10

2.2   NMR measurements

Silicon-29 NMR spectra were obtained on a Varian Inova 500 (Lakehead University), Bruker AMX 500 (University of Manitoba)   and Varian Inova 750 (Keck NMR Facility, University of Illinois at Urbana-Champaign) spectrometers operating at 99.28, 99.31 and 149.00 MHz, respectively. Glass coil supports in the AMX 500 probe head were replaced with Vespel SP-1 polyimide components in order to eliminate ^{29}Si background signals.

Chemical shifts are reported relative to tetramethylsilane, employing the orthosilicate monomer peak set to -71.0 ppm as a secondary reference. Carbon-13 and ^{1}H NMR spectra were obtained at 125.67 and 499.72 MHz, respectively, on the Varian Inova 500 spectrometer. Attention was paid to avoid sample contamination by contact with glass surfaces, and all samples were contained in custom 10 mm Kel-F NMR tubes (9 mm I.D.) or Teflon FEP-lined glass NMR tubes (8 or 4 mm I.D.). The detailed spectral parameters are provided in the individual figure captions. Spectra were usually acquired both with and without ^{1}H decoupling, gated to avoid NOE effects. Boron-11 NMR was acquired with the Varian Inova 500 spectrometer. The bottom was removed from the borosilicate NMR tube in order to eliminate the corresponding broad background signals.

11

2.3 Speciation of pentaoxosilicon complexes formed with glucoheptonic acid

Table 2.2 lists the samples which were prepared to investigate pentaoxosilicon complexes of glucoheptonic acid using ^{29}Si NMR spectroscopy. Table 2.3 lists the samples used for running ^{13}C NMR spectra.

Table 2.2. Samples used to study pentaoxosilicon complexes of glucoheptonic acid using ^{29}Si NMR spectroscopy

Temperature (°C)	Concentration (mol kg^{-1})		
	SiO$_2$	NaOH	sodium glucoheptonate
27	1.00	1.00	1.26
27	0.998	0.948	2.06
10 & -5	1.00	3.50	1.72
-5	0.972	1.16	0.593
-5	1.00	1.20	2.11
-5	0.993 (^{29}Si)	1.19	2.11

Table 2.3. Samples used to study pentaoxosilicon complexes of glucoheptonic acid using ^{13}C NMR spectroscopy (at -5 °C)

Concentration (mol kg^{-1})			pH
SiO$_2$	NaOH	sodium glucoheptonate	
0.993 (^{29}Si)	1.19	2.11	12.28
0	1.20	2.10	12.21

12

2.4 Speciation of hexaoxosilicon complexes formed with acyclic polyols

The samples used to investigate the structure of hexaoxosilicon complexes formed with acyclic polyol ligands are listed in Table 2.4. Silicon-29 NMR spectra were acquired at -5 °C.

Table 2.4. Samples used to study hexaoxosilicon complexes of acyclic polyols

Concentration (mol kg^{-1})			pH
SiO$_2$	NaOH	Ligand	
1.36	2.72	potassium gluconate, 2.04 potassium hydrogen saccharate, 2.04	13.365
1.33	2.66	potassium gluconate, 3.99	12.998
1.36	7.00	potassium hydrogen saccharate, 4.08	13.258

2.5 Speciation of hexaoxosilicon complexes formed with furanoidic vicinal cis-diols

The samples used to investigate the structure of hexaoxosilicon complexes formed with furanoidic vicinal cis-diol ligands are listed in Table 2.5. Silicon-29 NMR spectra were acquired at -5 °C.

13

Table 2.5. Samples used to study hexaoxosilicon complexes formed with furanoidic vicinal cis-diols

Concentration (mol kg^{-1})		
SiO$_2$	**NaOH**	**Ligand**
0.43	1.72	guanosine, 0.43 adenosine, 0.43
0.43	1.72	guanosine, 0.86
0.43	1.72	adenosine, 0.86
0.43	1.72	guanosine, 0.43 uridine, 0.43
0.43	1.72	guanosine, 0.43 cytidine, 0.43
0.43	1.72	adenosine, 0.86 cytidine, 0.86
0.43	1.72	guanosine, 0.86 adenosine, 0.86
0.43	1.72	adenosine, 0.86 uridine, 0.86

14

2.6   Stability constants for boron and silicon diester complexes

The stability constants of complexes formed between aqueous silicon or aqueous boron and (a) D-arabitol, (b) 1,4-anhydroerythritol, (c) gluconic acid, (d) *cis*-1,2-cyclopentanediol or (e) guanosine hydrate were determined using ^{29}Si and ^{11}B NMR spectroscopy.

Two complete sets of silicate samples were prepared, one with NaOH : SiO$_2$ = 1.0:1 and the other with NaOH : SiO$_2$ = 3.0:1. (See Table 2.6.) The samples were then adjusted to pH 12.3 at 22 °C by addition of 36.7% HCl. Silicon-29 NMR spectra were then recorded at 22 °C on the Bruker AMX 500 spectrometer (with silicon-free probe and sample tube). Two more sets of samples, identical to those just described, were adjusted to pH 12.2 at 0 °C and ^{29}Si NMR spectra recorded at 2 °C. (See Table 2.7.)

A single set of borate samples was prepared and adjusted to pH 12.0 at 24 °C by addition of 36.7% HCl. (See Table 2.8.) Boron-11 NMR spectra were recorded at 24 °C using the Varian Inova 500 spectrometer.

Table 2.6.   Samples prepared for determining the stability constants of silicon

complexes at 22 °C

NaOH : SiO₂	Adjusted pH	Concentration (mol kg⁻¹)	
		SiO₂	Ligand
3:1	12.30	1.00	D-arabitol, 2.50
1:1	12.30	0.992	D-arabitol, 2.48
3:1	12.30	0.916	1,4-anhydroerythritol, 2.36
1:1	12.30	0.972	1,4-anhydroerythritol, 2.22
3:1	12.30	0.891	gluconic acid, 2.23
1:1	12.30	1.02	gluconic acid, 2.32
3:1	12.29	0.902	1,2-cyclopentanediol, 2.30
1:1	12.30	0.980	1,2-cyclopentanediol, 2.24
4.3:1	12.00	0.43	guanosine, 0.851

16

Table 2.7. Samples prepared for determining the stability constants of silicon complexes at 0 °C

NaOH : SiO$_2$	Adjusted pH	Concentration (mol kg^{-1})	
		SiO$_2$	Ligand
3:1	12.15	0.95	D-arabitol, 2.38
1:1	12.19	0.95	D-arabitol, 2.37
3:1	12.20	0.96	1,4-anhydroerythritol, 2.66
1:1	12.19	0.96	1,4-anhydroerythritol, 2.45
3:1	12.20	0.87	gluconic acid, 2.18
1:1	12.19	0.94	gluconic acid, 2.36
3:1	12.19	0.89	1,2-cyclopentanediol, 2.28
1:1	12.01	0.91	1,2-cyclopentanediol, 2.35
4.3:1	12.01	0.43	guanosine, 0.85
4:1	12.00 [a]	0.43	guanosine, 0.85

[a] NMR for this particular sample was run at –5 °C.

Table 2.8. Samples prepared for determining the stability constants of boron

complexes at 24 °C

NaOH : H_3BO_3	Adjusted pH	Concentration (mol kg^{-1})	
		H_3BO_3	Ligand
4:1	12.05	0.11	D-arabitol, 0.11
4:1	12.06	0.10	1,4-anhydroerythritol, 0.10
4:1	12.00	0.10	gluconic acid, 0.10
4:1	12.01	0.11	1,2-cyclopentanediol, 0.12
4:1	12.00	0.11	guanosine, 0.11
3:1	12.06	0.1 (external reference)	

18

Chapter 3 – Results and Discussion

3.1 The structure of pentaoxosilicon complexes formed with acyclic polyols

Figure 3.1.1 shows ^{29}Si NMR spectra of three characteristic acyclic polyol and furanoidic *cis*-diol silicate solutions, expanded to show the penta-coordinate silicon region. Pentaoxo Si complexes formed by furanoidic *cis*-diol ligands such as anhydroerythritol are typically represented by three pentet ^{29}Si NMR resonances in the –97.2 to –98.6 ppm region, clearly showing that that each Si centre is coupled to four nearly-equivalent hydrogens via Si-O-C-H ester linkages (Figure 3.1.1a). Detailed structural analysis reveals that all three complexes are monomeric and contain two bidentate ligands [55]. By comparison, the pentaoxo Si complexes formed with acyclic polyol ligands generally yield several exchange-broadened resonances that are located at the upfield end of the penta-coord Si region (–100.5 to –102.4 ppm) and lack resolvable fine structure from ^{1}H-^{29}Si coupling (Figure 3.1.1.b) [39, 54].

Glucoheptonic acid, however, is an acyclic polyol ligand that yields both types of ^{29}Si resonances, that is, a well-resolved pentet at the high frequency end of the penta-coord Si region plus exchange-broadened resonances at the low frequency end (Figure 3.1.1c) [48]. Moreover, additional multiplet resonances appear which would suggest the existence of complexes containing as few as two ester linkages at the silicon centre.

In this study, we examined the glucoheptonic acid system more fully in hope of ascertaining the structures of pentaoxo silicon complexes formed with acyclic

19

polyols. The first task was to find solution conditions which optimize the appearance

of strong signals in the 5-coord Si region of the ^{29}Si NMR spectrum. Formation of

pentaoxo Si complexes is favoured at high ligand concentrations (Figure 3.1.2) and

low temperature (Figure 3.1.3). Ultimately, we determined the optimum solution

condition to be 1.0 mol kg^{-1} SiO$_2$, 1.2 mol kg^{-1} NaOH, 2.1 mol kg^{-1} sodium

glucoheptonate and –5 °C, as demonstrated in Figure 3.1.4.
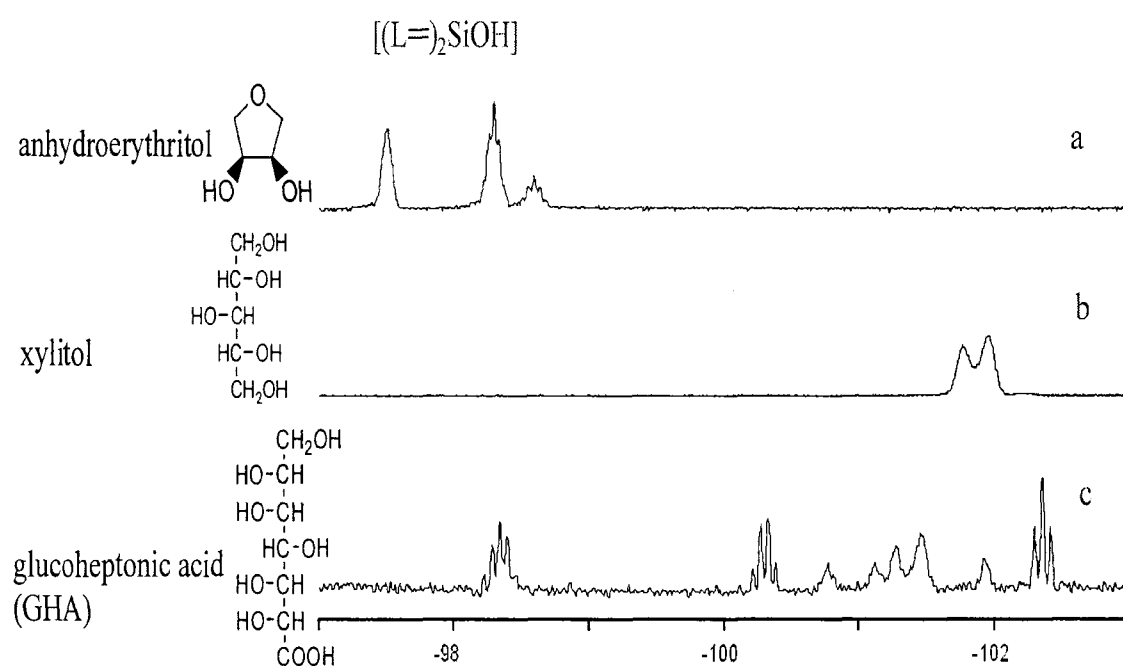
Figure 3.1.1. Silicon-29 NMR (99.36 MHz) ^{1}H-coupled spectra, expanded to show

the 5-coord Si region, of aqueous solutions containing: (a) 0.5 mol kg^{-1} SiO$_2$, 0.65

mol kg^{-1} NaOH and 4.0 mol kg^{-1} anyhydroerythritol at 5 °C; (b) 1.75 mol % of both

SiO$_2$ and NaOH, and 12.5 mol % xylitol at 7 °C; (c) 0.95 mol kg^{-1} of both SiO$_2$ and

NaOH, and 1.4 mol kg^{-1} sodium glucoheptonate at 27 °C.
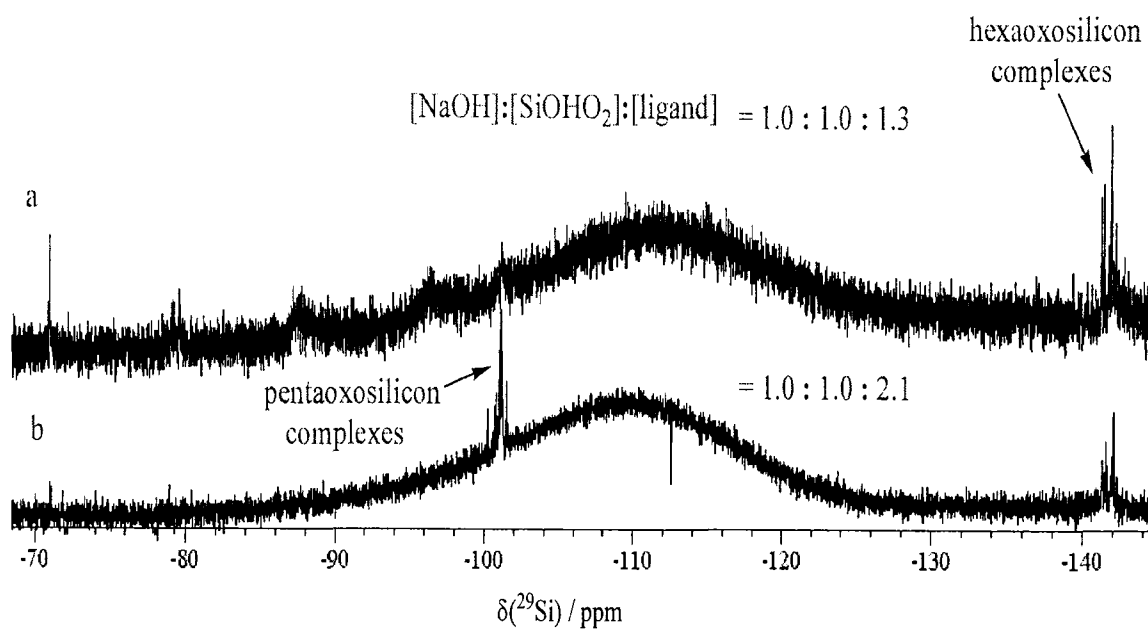
Figure 3.1.2. Silicon-29 NMR (99.36 MHz) ^{1}H-decoupled spectra of aqueous

solutions at 27 °C containing: (a) 1.0 mol kg^{-1} SiO$_2$, 1.0 mol kg^{-1} NaOH and 1.26 mol

kg^{-1} sodium glucoheptonate; or (b) 1.0 mol kg^{-1} SiO$_2$, 1.0 mol kg^{-1} NaOH and 2.1

mol kg^{-1} sodium glucoheptonate.

21
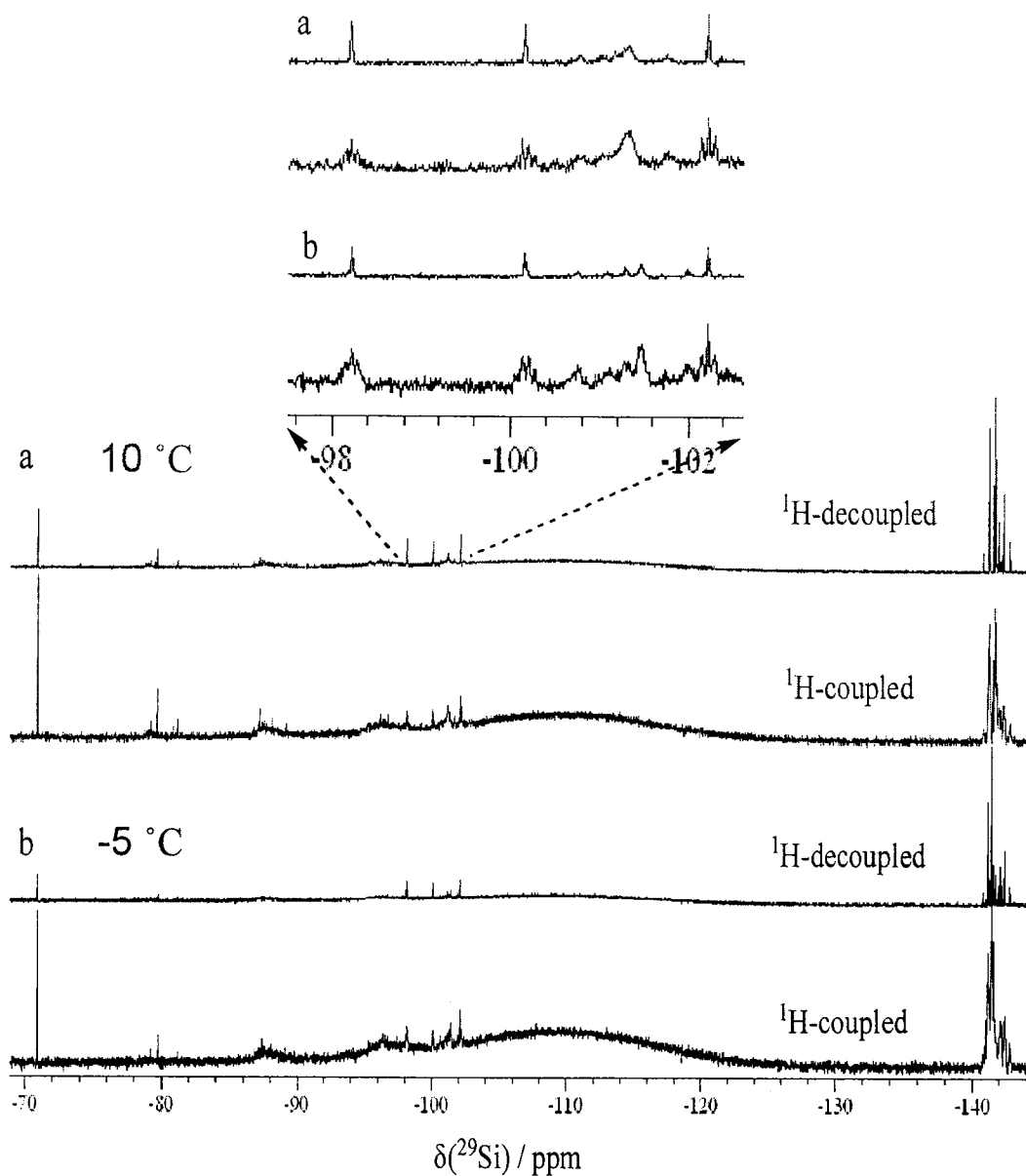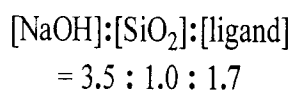
Figure 3.1.3. Silicon-29 NMR (99.36 MHz) ^{1}H-decoupled and coupled spectra of

aqueous solutions containing 1.0 mol kg^{-1} SiO$_2$, 3.5 mol kg^{-1} NaOH and 1.7 mol kg^{-1}

sodium glucoheptonate at (a) 10 °C and (b) –5 °C.

pentaoxosilicon complexes

hexaoxosilicon complexes

δ(²⁹Si)/ppm
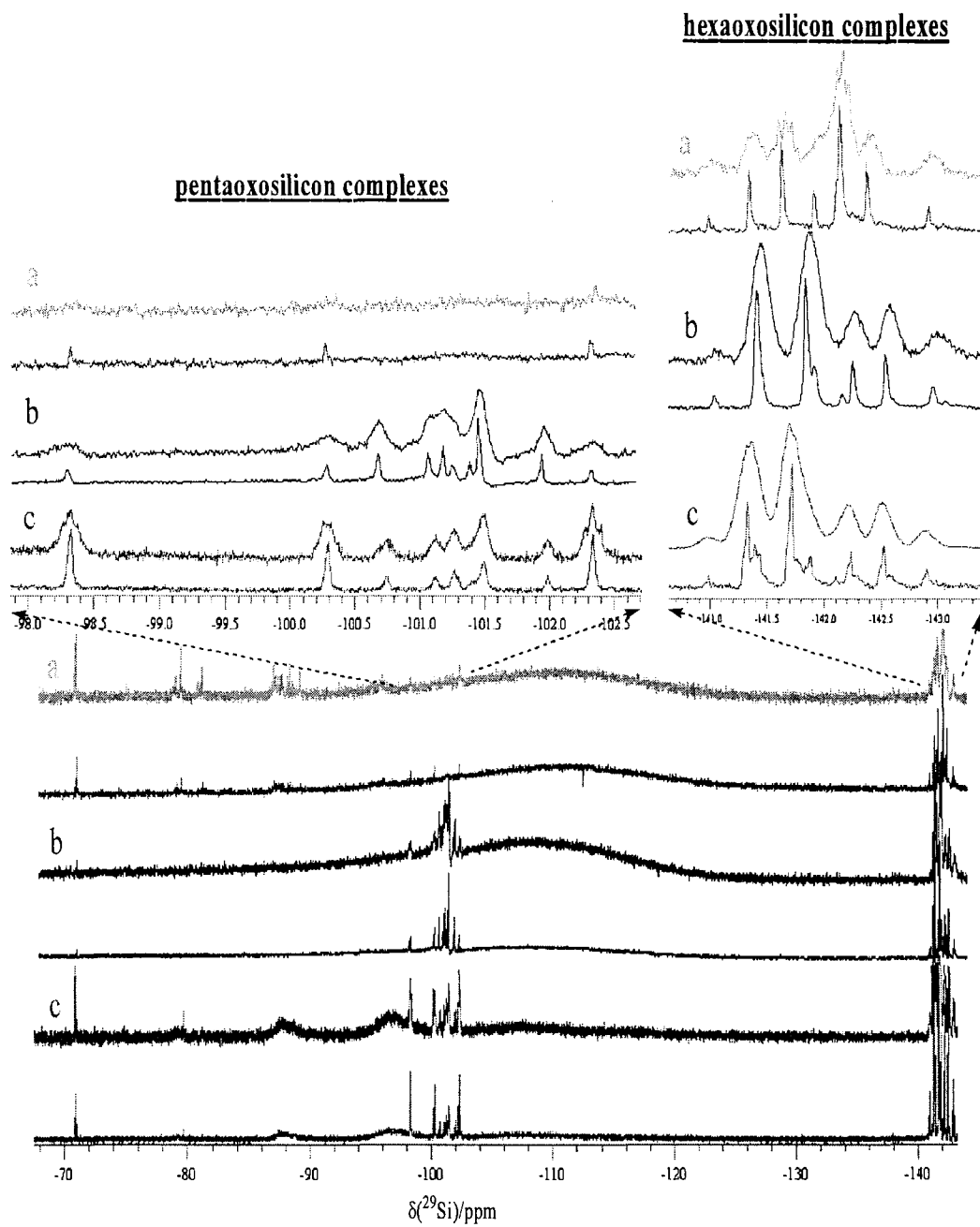
Figure 3.1.4. Silicon-29 NMR (99.36 MHz) ¹H-decoupled and coupled spectra of

aqueous solutions at –5 °C containing: (a) 1.0 mol kg⁻¹ SiO₂, 1.16 mol kg⁻¹ NaOH and

0.6 mol kg⁻¹ sodium glucoheptonate; (b) 1.0 mol kg⁻¹ SiO₂, 1.16 mol kg⁻¹ NaOH and

2.1 mol kg⁻¹ sodium glucoheptonate; or (c) 1.0 mol kg⁻¹ ²⁹SiO₂ (99% isotopic

enrichment), 1.16 mol kg⁻¹ NaOH and 2.1 mol kg⁻¹ sodium glucoheptonate.

23

Although glucoheptonic acid produces exchange broadened ^{29}Si NMR signals in the -100.5 to -102.2 ppm region as observed for other non-cyclic polyol ligands such as xylitol, sorbitol, saccharic acid and gluconic acid, it also yields three resonances centred at –98.3, –100.3 and –102.4 ppm, which exhibit distinct ^{1}H-^{29}Si splitting patterns. (See Table 3.1). As shown in Figure 3.1.3, these peak positions are reasonably temperature independent. The relative positions and splitting patterns of the three equally spaced multiplets provide insight into the structure of the corresponding complexes. The pentet at –98.3 ppm has a chemical shift and J-coupling very near to that of the pentets that are characteristic of furanoidic cis-diol Si complexes [54, 55] and, therefore, similarly corresponds to a complex with four Si-O-C-H ester linkages at its silicon centre. The quartet at –100.3 ppm is consistent with a structure in which silicon has three ester linkages. Finally, the triplet at –102.4 ppm corresponds to a complex containing two silicon ester linkages.

Carbon-13 NMR spectroscopy was employed to determine the location of the glucoheptonic acid coordination sites in these complexes. In accordance with the previously established binding rules for acyclic polyols [39, 44], the expected Si-diester formation sites on glucoheptonic acid are the *threo* hydroxy groups at carbons C_3/C_4 and C_4/C_5 (Figure 3.1.5). Analysis of ^{13}C NMR spectra obtained of alkaline glucoheptonate solutions in the presence and absence of dissolved silica (Figure 3.1.6) reveals the following.

24

Table 3.1. ^{29}Si NMR assignments for the pentaoxosilicon glucoheptonic acid complexes [a]

Species	δ (^{29}Si) [b] /ppm	Multiplicity [$^{3}J(^{29}$Si-O-C-^{1}H) /Hz]
[η^2-2,3,4,5-(+)-glucoheptonato]silicate [(L$\equiv$) Si OH]$^-$	−98.3	pentet [5.6]
[η^2-3,4,5-(+)-glucoheptonato]silicate [(L$=$) Si (OH)$_2$]$^-$	−100.3	quartet [6.8]
[η^2-3,4-(+)-glucoheptonato]silicate ([(L$=$) Si (OH)$_3$]$^-$	−102.35	triplet [7.4]
Other [(L$=$)$_2$SiOH]$^-$ species	−100.68	indeterminate
	−101.1	indeterminate
	−101.2	indeterminate
	−101.26	indeterminate
	−101.4	indeterminate
	−101.5	indeterminate
	−102.0	indeterminate

[a] Chemical shift and coupling constants are dependent on solution conditions and here correspond to a solution containing 0.99 mol kg^{-1} SiO$_2$, 1.2 mol kg^{-1} NaOH and 2.11 mol kg^{-1} sodium glucoheptonate at 269 K. [b] Chemical shift from tetramethylsilane, employing the orthosilicate monomer peak (assigned here at −71 ppm) as a secondary reference.

CH_2OH 1

$HO-CH$ 2

$HO-CH$ 3

$HC-OH$ 4

$HO-CH$ 5

$HO-CH$ 6

$COOH$ 7
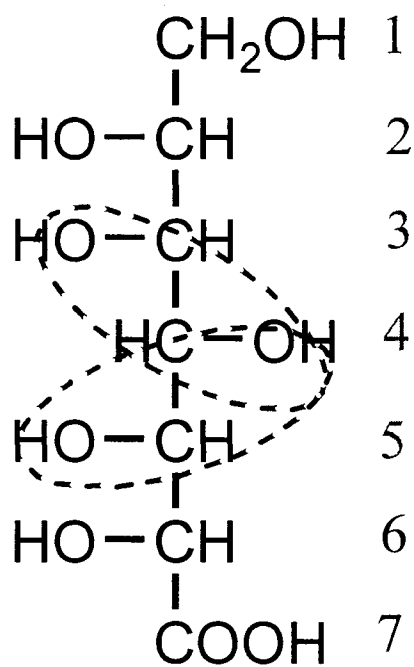
Figure 3.1.5.   The Fischer projection of glucoheptonic acid, showing the two *threo*

pairs of hydroxy groups which are potential sites for Si diester formation in

accordance with the established Si-bonding rules for acyclic polyols [43, 47]. Thus,

the C_4 hydroxy group is expected to be a common Si-binding site in all complexes.
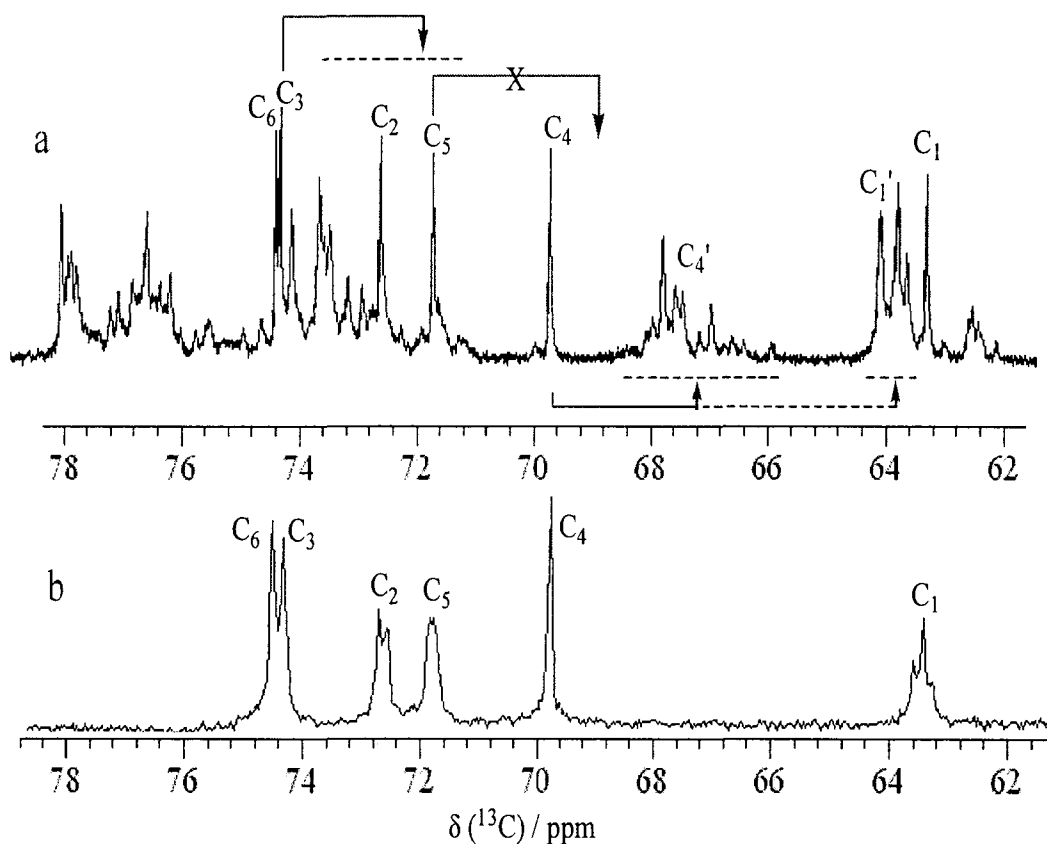
Figure 3.1.6. Carbon-13 (125.66 MHz) ^{1}H-decoupled NMR spectrum of aqueous

solutions at –5 °C containing: (a) 1.0 mol kg^{-1} enriched SiO_2, 1.2 mol kg^{-1} NaOH and

2.1 mol kg^{-1} sodium glucoheptonate; (b) 1.2 mol kg^{-1} NaOH and 2.0 mol kg^{-1} sodium

glucoheptonate. Peaks corresponding to carbons 1-6 of glucoheptonic acid are

labeled accordingly. (Refer to Figure 3.1.5.) The peaks labeled C_1' and C_4'

correspond to silicon-complexed ligands. The arrows indicate the shift of carbon

resonances due to the formation of the silicon complexes with glucoheptonate.

(1) As expected, the C_4 hydroxy group is a Si binding site in every pentaoxo Si-

glucoheptonate complex in solution. Spectral integration shows that all C_4' peaks –

i.e., peaks corresponding to C_4 in ligands that are bound to Si – are located on the

low-frequency side of the "free" C_4 resonance, consistent with the strong shielding

influence of –OSi groups [55]. Comparison of the integration data with those

obtained from corresponding ^{29}Si NMR spectra reveals that the peaks clustered

between 1.2 and 3.6 ppm up-field of the "free" C_4 resonance account for *ca.* 24.4% of

the total C_4' concentration in solution. The remaining 6.1 % of C_4' carbons are even

more shielded, with their peaks shifted well into the C_1 region.

(2) The C_5 hydroxy group is evidently a minor Si-binding site since there are no

significant resonances corresponding to C_5' located anywhere up-field within 3.8 ppm

of the "free" C_5 peak. This is supported by ^{13}C NMR integration. Consequently, it is

the C_3/C_4 *threo* pair of hydroxy groups that represents the principal location of silicate

diester formation in every Si-glucoheptonate complex .

(3) Ligand complexation leads to C_1' peaks appearing on both sides of the "free" C_1

resonance, although the majority appear to be shifted down-field. However, the up-

field peaks are shifted only slightly in comparison with the C_4' resonances, indicating

that the few Si-O-C linkages formed at this site are relatively weak. By contrast, a

relatively high fraction of the C_6' resonances appear up-field of the "free" C_6 peak,

indicating that (a) the C_6 hydroxy groups participate in ester link formation, and (b)

they are more important in this regard than C_1. Thus, both tri- and tetra-ester

complexes result when the hydroxy groups at C_6 and/or C_1 participate with the C_3/C_4

threo pair in binding to silicon. This is consistent with coexistence of triplet, quartet

and pentet ^{29}Si resonances having characteristic scalar $^3J(^{29}\text{Si-O-C-}^1\text{H})$ three-bond

28

coupling constants between 5.5 and 7.5 Hz. As would be expected, the coupling strength decreases as the number of ester linkages at the Si centre rises.

Glucoheptonic acid has a unique configuration of hydroxy groups that enable it to surround silicon with each hydroxy group directed inwards, as shown in Figure 3.1.7. With silicon bound to the hydroxy groups at C_3/C_4, the groups at C_1 and C_6 readily adopt approximate trigonal bipyramidal coordination positions, providing support for the ^{29}Si and ^{13}C NMR findings. The triplet, quartet and pentet ^{1}H-coupled ^{29}Si NMR resonances would therefore correspond to monomeric species $[L=Si(OH)_3]^-$, $[L{\equiv}Si(OH)_2]^-$ and $[L{\equiv}SiOH]^-$, respectively, where L = glucoheptonate ligand. Based on the NMR evidence, we conclude that the ester linkages in $[L=Si(OH)_3]^-$ occur at ligand sites C_3/C_4, while in $[L{\equiv}SiOH]^-$ they occur at $C_1/C_3/C_4/C_6$. The NMR evidence is insufficient to determine with certainty if the ester links in $[L{\equiv}Si(OH)_2]^-$ are at $C_1/C_3/C_4$ or $C_3/C_4/C_6$. The ^{29}Si NMR resonances of these three solution species exhibit very little exchange broadening compared with those of other known pentacoordinated silicon complexes formed with acyclic polyol ligands [48]. The implied kinetic stability is attributable to the efficient intramolecular H-bonding network established when all glucoheptonate hydroxy groups are oriented towards the Si centre. Moreover, the ligand's outward-facing hydrocarbon backbone is expected to yield significant hydrophobic stabilization of the complex from subsequent hydrolysis [52].

In addition to the three well-resolved ^{29}Si NMR multiplets discussed above, the pentaoxosilicon spectral region contains up to ten or more exchange-broadened

29

resonances between -100.5 and -102.2 ppm. (See Figures 3.1.4 and 3.1.7.) The chemical shift range and broadened appearance of these resonances is analogous to that of pentacoordinated ^{29}Si NMR resonances observed for all other acyclic polyol ligands known to complex silicon. (Compare, for example, the case of xylitol in Figure 3.1.1.) We have previously determined that the complexes corresponding to these broad signals are monomeric and possess a 2:1 ligand-to-silicon ratio [44, 55]. Glucoheptonic acid yields a larger number of such $[L_2 \equiv SiOH]^-$ complexes compared, *e.g.*, with xylitol because of the multitude of bonding configurations this ligand provides. The lability of all polyol $[L_2 \equiv SiOH]^-$ complexes is clearly higher than $[L_2 \equiv SiOH]^-$ species formed with furanoidic *cis*-diols and also than the mono-glucoheptonate complexes discussed above. Moreover, the ^{29}Si NMR chemical shifts are anomalously low compared with other Si tetraester complexes (Figures 3.1.1 and 3.1.7), indicating that the ester linkages in these species are significantly weakened by steric interaction between their two coordinating polyol ligands.

30
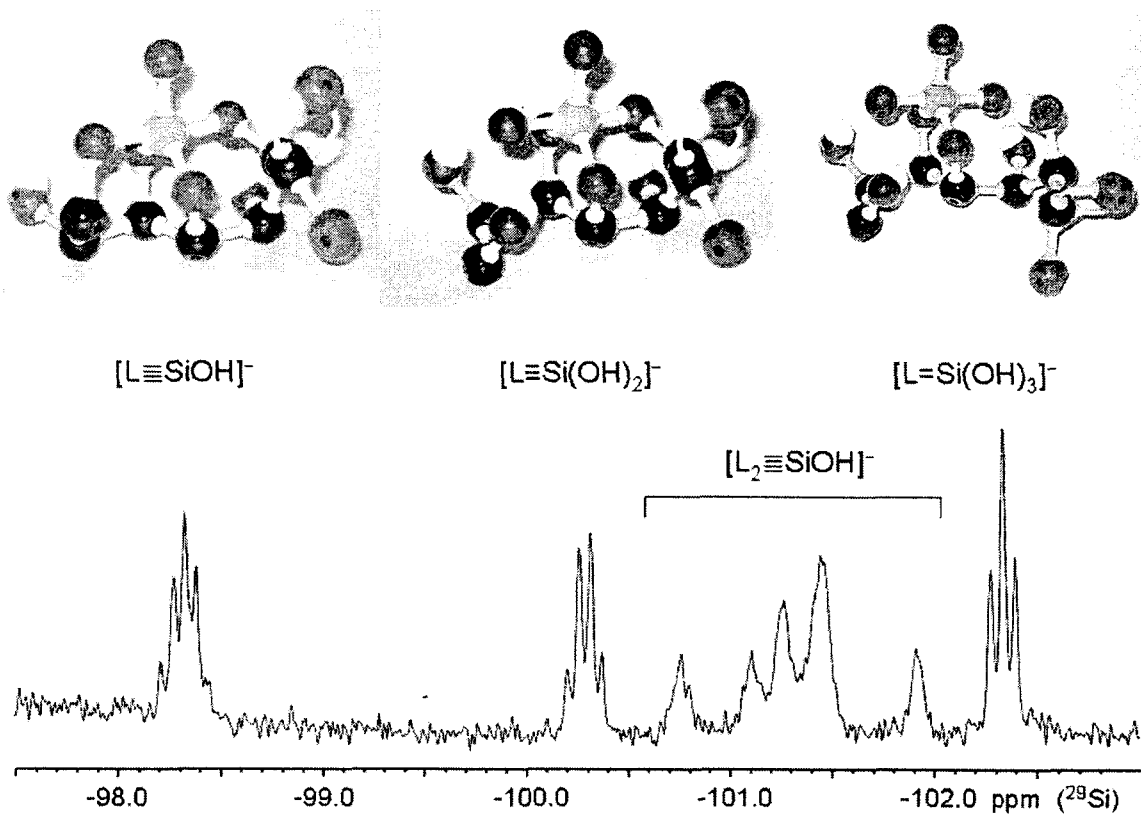
Figure 3.1.7. Models of Si-glucoheptonate diester, triester and tetraester complexes.

The blue, red and black atoms represent Si, O and C, respectfully.

3.2 The structure of hexaoxosilicon complexes formed with acyclic polyols

Hexaoxosilicon complexes formed with acyclic polyols yield ^{29}Si NMR resonances in the -140 to -145 ppm chemical shift region (Figure 1.1). Two complexes are typically evident, each having a 3:1 ligand-to-silicon ratio [39, 48, 50]. To facilitate their structural characterization we prepared aqueous silicate solutions containing D-gluconic acid and/or D-saccharic acid. Both ligands are strong Si-binders and contain just one *threo* pair of hydroxy groups (Figure 3.2.1). Moreover, the hexaoxosilicon complexes that they form have distinctly different ^{29}Si NMR chemical shifts.
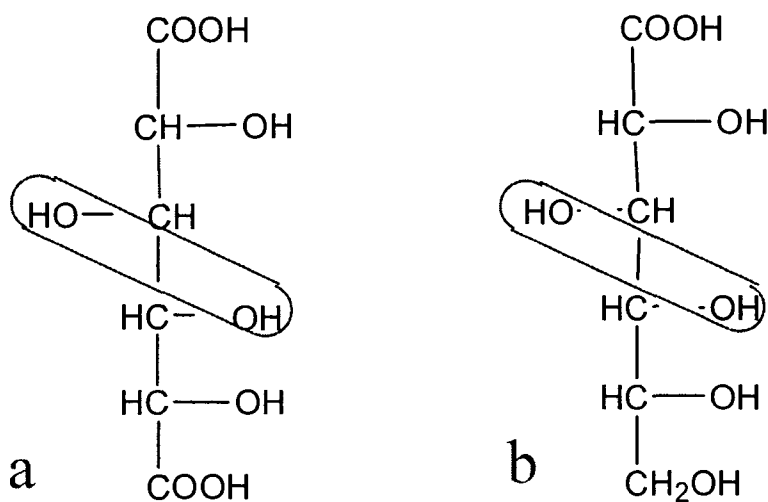
Figure 3.2.1. Fischer projections of (a) D-saccharic acid and (b) D-gluconic acid. Each ligand contains a *threo* pair of hydroxy groups (circled) flanked by two other hydroxy groups, creating a single binding site for silicon.

Figures 3.2.2 (a) and (b) show the ^{29}Si NMR spectra of equivalent silicate solutions containing D-saccharic acid and D-gluconic acid, respectively. When saccharic acid is present, two resonances appear in the 6-coord Si spectral region at -140.04 and -141.88 ppm. Gluconic acid similarly yields two peaks at -142.18 and -142.62 ppm. Integration of the corresponding ^{29}Si and ^{13}C NMR spectra indicates that all four resonances represent monomeric $[SiL_3]^{2-}$ silicate complexes, each containing three bidentate ligands. The coexistence of two such species in each solution would suggest they are inequivalent diastereomers, that is, one having all three ligands oriented in a single direction ($L_\delta L_\delta L_\delta$) and the other with one ligand reversed ($L_\delta L_\delta L_\lambda$) (Scheme 1). The latter species would be sterically hindered somewhat, which leads us to assign the $L_\delta L_\delta L_\lambda$ diastereomer to the upfield resonances in Figures 3.2.2 (a) and (b) owing to the lower signal intensities.

Our structural hypothesis was tested by preparing a silicate solution containing both gluconic acid and saccharic acid. If the above interpretation is correct, this system should yield twelve different $[SiL_3]^{2-}$ species: two GGG diastereomers (containing three gluconic acids); two SSS diastereomers (containing three saccharic acids); four GGS diastereomers; and four SSG diastereomers. The ^{29}Si NMR spectrum of this solution, shown in Figure 3.2.2 (c), does indeed exhibit twelve distinct resonances in the 6-coord Si region. Two resonances at -140.04 and -141.84 ppm correspond to the $S_\delta S_\delta S_\delta$ and $S_\delta S_\delta S_\lambda$ diastereomers. The resonances at -142.18 and -142.68 ppm correspond to $G_\delta G_\delta G_\delta$ and $G_\delta G_\delta G_\lambda$. The remaining eight resonances can be divided into two groups. One group represents complexes

33

containing one gluconate and two saccharate ligands: $G_\delta S_\delta S_\delta$; $G_\lambda S_\delta S_\delta$; $G_\delta S_\delta S_\lambda$; and

$G_\lambda S_\lambda S_\delta$. The other group represents species with one saccharate and two gluconate

ligands: $G_\delta G_\delta S_\delta$; $G_\delta G_\delta S_\lambda$; $G_\delta G_\lambda S_\delta$; and $G_\delta G_\lambda S_\lambda$.

$$L_\delta L_\delta L_\delta \qquad L_\delta L_\delta L_\lambda$$
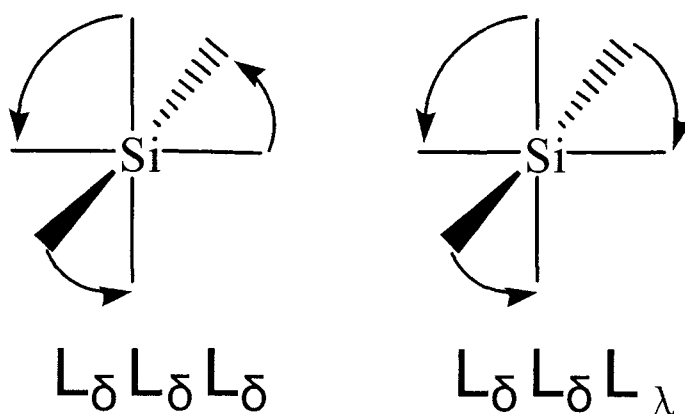
Scheme 1. The two diastereomers of $[SiL_3]^{2-}$.
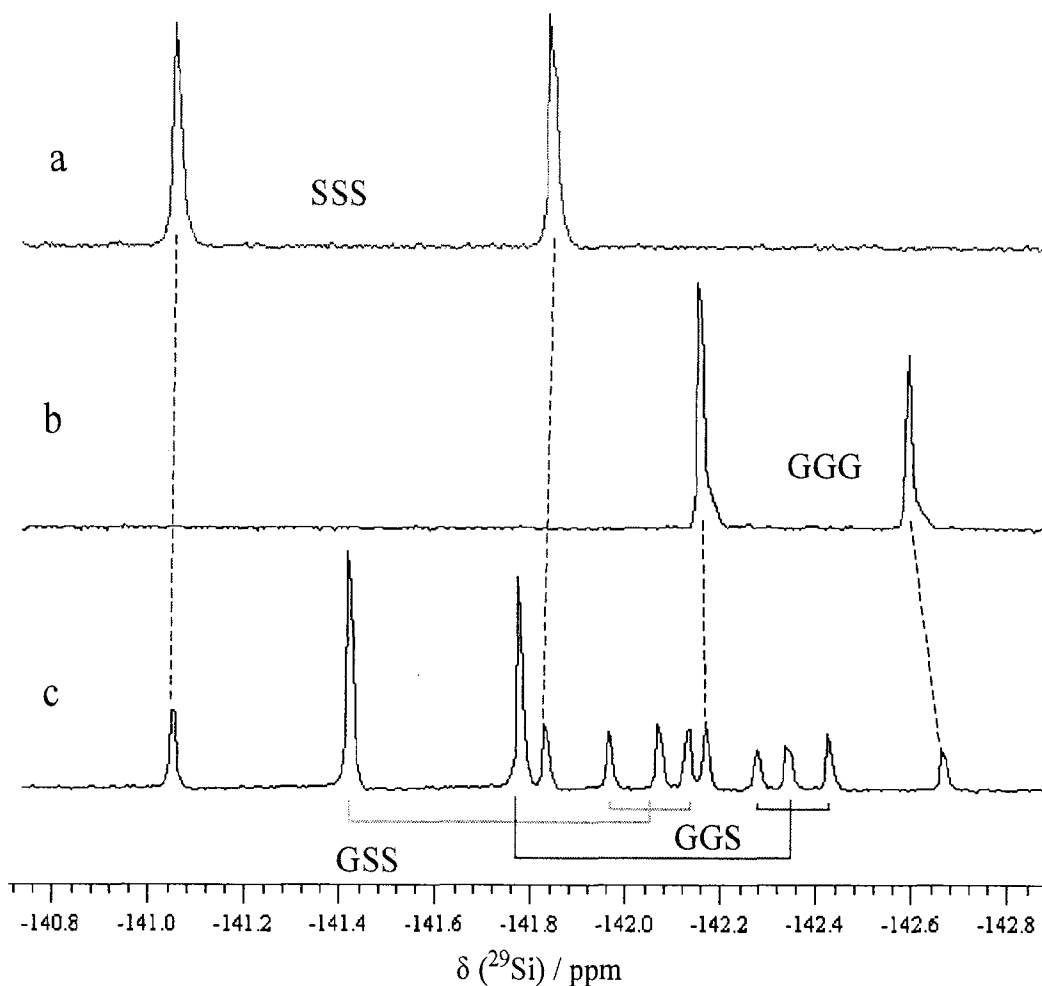
Figure 3.2.2. Silicon-29 NMR (99.36 MHz) spectra of aqueous solutions at −5 °C

containing (a) 1.36 mol kg^{-1} SiO$_2$, 6.82 mol kg^{-1} NaOH and 4.10 mol kg^{-1} D-

saccharic acid monopotassium salt; (b) 1.33 mol kg^{-1} SiO$_2$, 2.66 mol kg^{-1} NaOH and

4.05 mol kg^{-1} potassium D-gluconate; and (c) 1.36 mol kg^{-1} SiO$_2$, 2.75 mol kg^{-1}

NaOH, 2.04 mol kg^{-1} D-saccharic acid monopotassium salt and 2.06 mol kg^{-1}

potassium D-gluconate. Each solution contains approximately equal concentrations of

SiO$_2$, OH$^-$ and ligand. Here, 'S' represents saccharic acid, 'G' represents gluconic

acid, and thus 'SGG' is used to represent a [SiL$_3$]$^{2-}$ complex containing one saccharic

acid ligand and two gluconic acid ligands.

35

3.3 The structure of hexaoxosilicon complexes formed with furanoidic *cis*-diol molecules

The hexaoxosilicon complexes formed with most furanoidic vicinal *cis*-diol ligands – *e.g.*, 1,4-anyhydroerythritol, guanosine, adenosine – yield two ^{29}Si NMR resonances in the −135 to −139 ppm spectral region (Figure 3.3.1) which, in accordance to ^{13}C and ^{29}Si NMR spectral integration data, correspond to two different $[SiL_3]^{2-}$ species (Figure3.3.2). (Ribose yields many more such species owing to the presence of two Si-binding sites Figure 3.3.3). The situation is exactly analogous to that of the acyclic polyol Si-complexes discussed in section 3.2, and therefore the two 6-coord Si-complexes can be identified with reasonable certainty as the $L_\delta L_\delta L_\delta$ and $L_\delta L_\delta L_\lambda$ diastereomers of $[SiL_3]^{2-}$.

In support of this conclusion, we find that bulky ligands such as guanosine and adenosine (Figure 3.3.4) significantly suppress the upfield ^{29}Si NMR resonance that we assign to the $L_\delta L_\delta L_\lambda$ diastereomer (Figure 3.3.5). Thus, guanosine (G) yields one major 6-coord ^{29}Si peak at −137.3 ppm from $G_\delta G_\delta G_\delta$, whereas adenosine (A) yields one peak at −138.3 ppm from $A_\delta A_\delta A_\delta$ (Figures 3.3.5a & b). Since the $L_\delta L_\delta L_\lambda$ diastereomers are severely hindered, one would logically predict that a solution that contains both of these bulky ligands would lead to a total of four 6-coord ^{29}Si resonances, corresponding to species $G_\delta G_\delta G_\delta$, $G_\delta G_\delta A_\delta$, $G_\delta A_\delta A_\delta$ and $A_\delta A_\delta A_\delta$. Instead, guanosine-adenosine mixtures consistently yield six large peaks in the hexaoxosilicon region at *ca.* −137.3, −137.5, −137.7, −138.0, −138.2 and −138.4 ppm (Figure 3.3.5c).

36
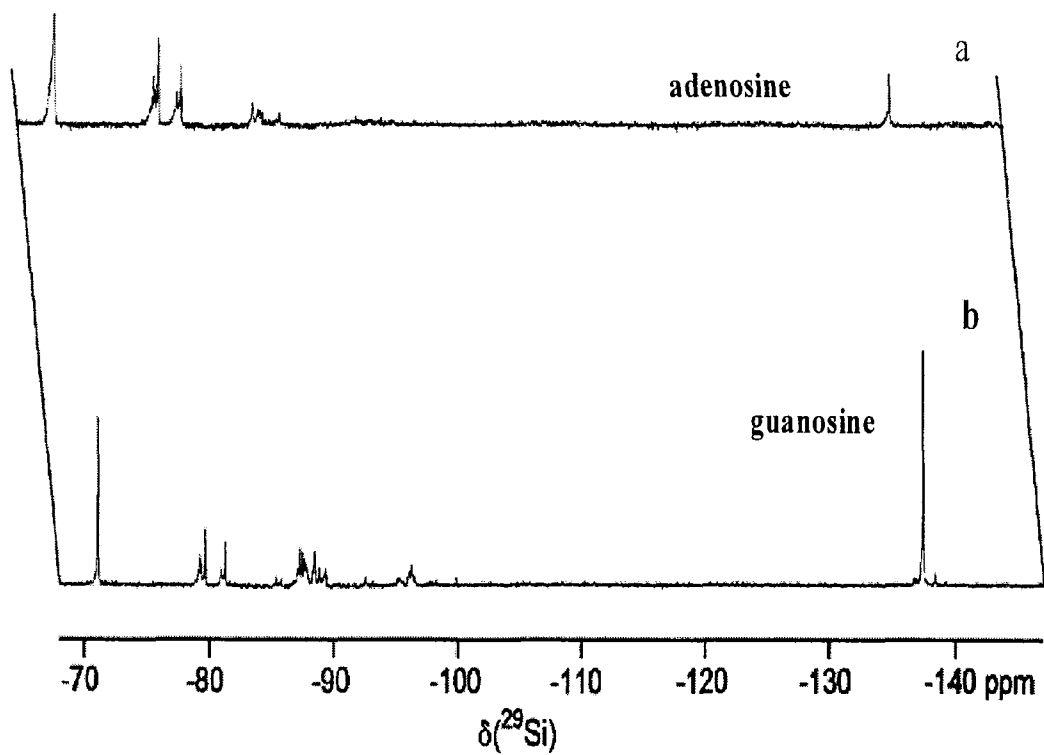
Figure 3.3.1. Silicon-29 NMR spectra of sodium silicate solutions containing 0.43

mol kg^{-1} SiO$_2$, 1.7 mol kg^{-1} NaOH and 0.86 mol kg^{-1} (a) adenosine; (b) guanosine at

5 °C.
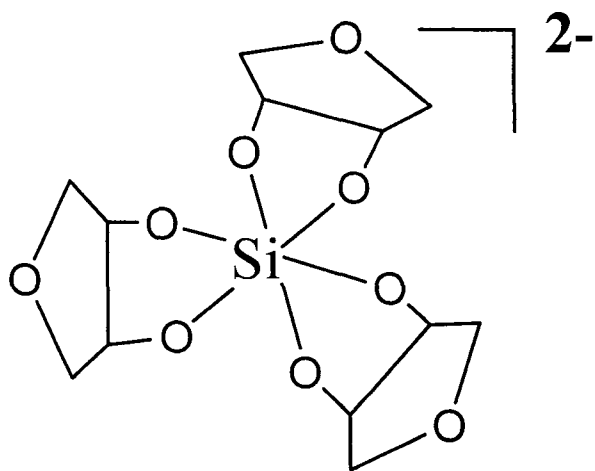
Figure 3.3.2. Structure of furanoidic hexaoxosilicon species [SiL$_3$]$^{2-}$
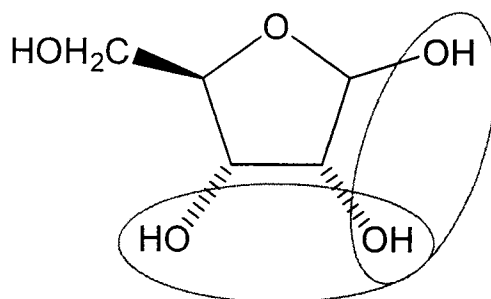
Figure 3.3.3. Structure of D-ribose showing the vicinal *cis*-diol groups that serve as bidentate Si-binding sites.

G   A

guanosine   adenosine
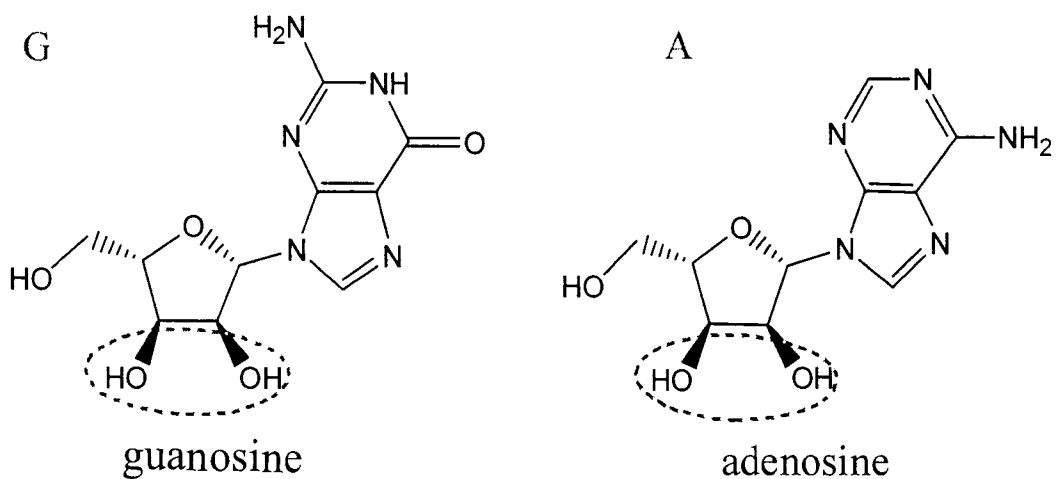
Figure 3.3.4. The structures of guanosine (G) and adenosine (A), showing the vicinal *cis*-diol groups that serve as bidentate Si-binding sites for these ligands.

38

a

b

c

-137.0   -137.2   -137.4   -137.6   -137.8   -138.0   -138.2   -138.4   -138.6

$\delta(^{29}\text{Si}) / \text{ppm}$
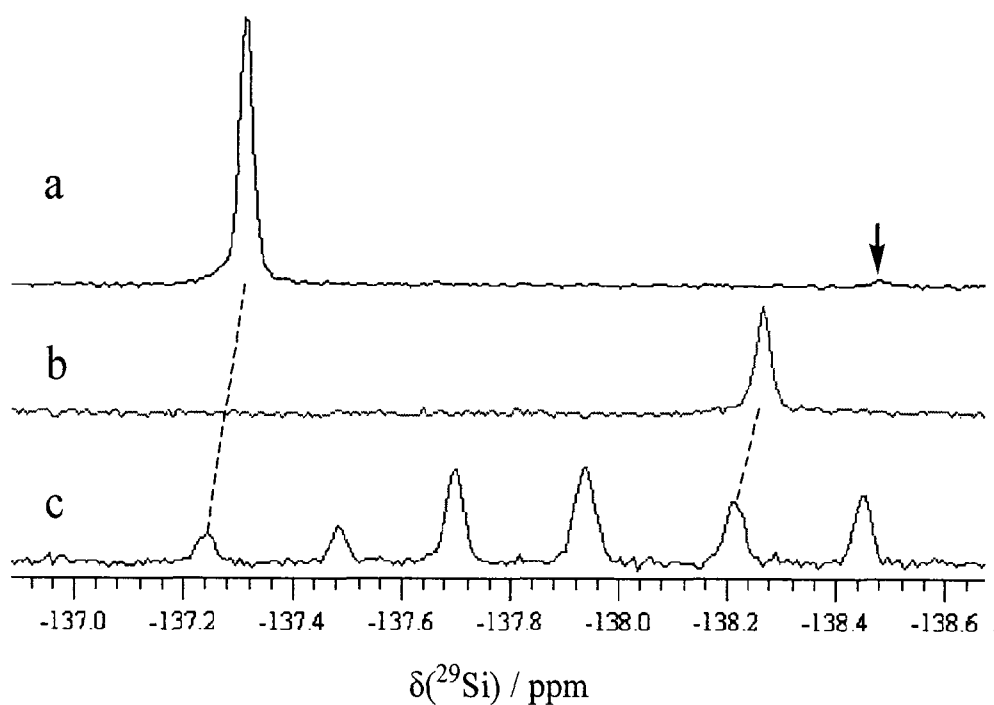
Figure 3.3.5. Silicon-29 NMR (99.36 MHz) spectra of the aqueous solutions at -5 °C

containing 0.43 mol kg^{-1} SiO$_2$, 1.72 mol kg^{-1} NaOH and: (a) 0.86 mol kg^{-1} guanosine;

(b) 0.86 mol kg^{-1} adenosine; (c) 0.43 mol kg^{-1} guanosine and 0.43 mol kg^{-1} adenosine.

Rudimentary molecular modeling, as presented in Figure 3.3.6, reveals that the

additional two resonances likely correspond to species G$_\delta$G$_\delta$A$_\lambda$ and A$_\delta$A$_\delta$G$_\lambda$ in which

adenosine and guanosine ligands are directed towards each other, with their aromatic

base groups positioned face-to-face, to form multi-point intramolecular H-bonding or

π-stacking. We have also investigated other ribonucleoside i.e., cytidine or uridine

combinated with guanosine or adenosine, the ^{29}Si NMR results are shown in Figure

3.3.7. As shown in Figure 3.3.7a and 3.3.7b, the combination of guanosine with

39

uridine or cytidine produces two ^{29}Si NMR resonances at -137.0 ppm and -137.4

ppm; it also produces some exchange-broadened ^{29}Si NMR signals in the -136.3 ppm

to -136.9 ppm region, where the strict guanosine, uridine or cytidine produces only

one ^{29}Si NMR resonance. Similarly the combination of adenosine with cytidine or

uridine, yields two ^{29}Si NMR resonances in the -137.7 to -138.0 ppm spectral region

(Figure 3.3.7c and 3.3.7e), and quite a few more exchange-broadened signals are

produced in the -136.0 ppm to -137.6 ppm region. All these results indicate that the

combination other ribonucleosides with either guanosine or adenosine yields the

similar effect as the combination of guanosine and adenosine (Figure 3.3.7d).
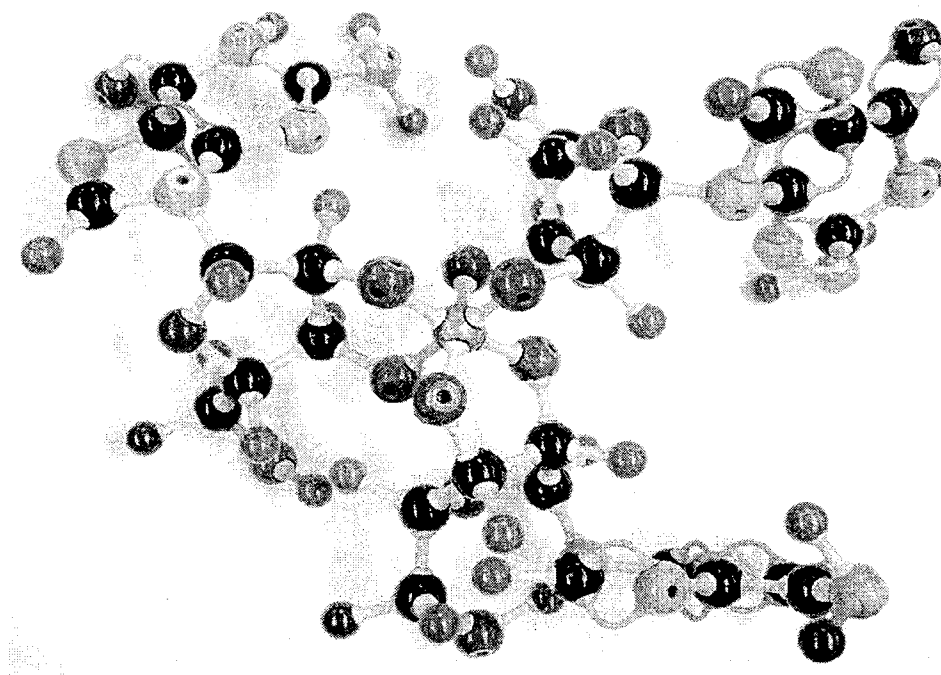
Figure 3.3.6. Molecular model of the guanosine-guanosine-adenosine $G_\delta G_\delta A_\delta$

hexaoxosilicon complex. Grey = Si, black = C, red = O and green = H.

40
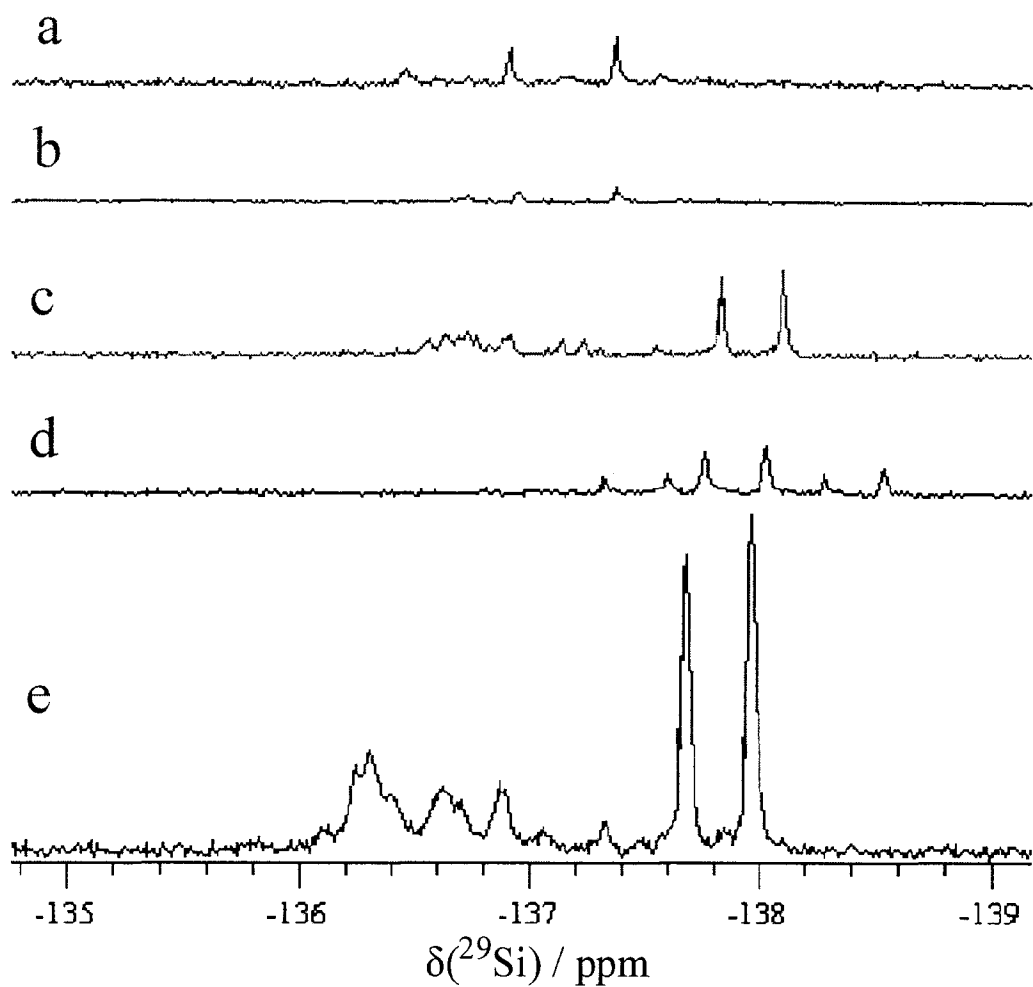
Figure 3.3.7. Silicon-29 NMR (99.36 MHz) spectra at −5 °C of aqueous solutions

containing 0.43 mol kg⁻¹ SiO₂, 1.72 mol kg⁻¹ NaOH and (a) 0.43 mol kg⁻¹ of each

guanosine and uridine; (b) 0.43 mol kg⁻¹ of each guanosine and cytidine; (c) 0.86 mol

kg⁻¹ of each adenosine and cytidine; (d) 0.86 mol kg⁻¹ of each guanosine and

adenosine; (e) 0.86 mol kg⁻¹ of each adenosine and uridine.

3.4 Stability constants for the silicon and boron complexes formed with acyclic polyol and furanoidic *cis*-1,2-diol ligands

A series of quantitative NMR experiments were carried out to determine the stability constants for representative acyclic polyol and furanoidic *cis*-1,2-diol complexes of aqueous silicon, and to compare the binding affinity of silicon to that of boron for these two types of ligands. The representative acyclic polyols chosen were D-arabitol and D-gluconic acid. For the furanoidic ligands, we selected *cis*-1,2-cyclopentanediol, 1,4-anhydroerythritol and guanosine.

Two sets of aqueous silicate solutions were prepared, each containing approximately 1.0 mol kg^{-1} SiO$_2$, 2.3 mol kg^{-1} ligand, and either 1.0 or 3.0 mol kg^{-1} NaOH. The solutions were then carefully pH adjusted (using microliter additions of 10.14 mol kg^{-1} HCl) to either pH 12.30 ± 0.01 at 22 °C or 12.20 ± 0.01 at 0 °C. Silicon-29 NMR spectra of all the solutions are shown in Fig. 3.4.1 to 3.4.5.

42
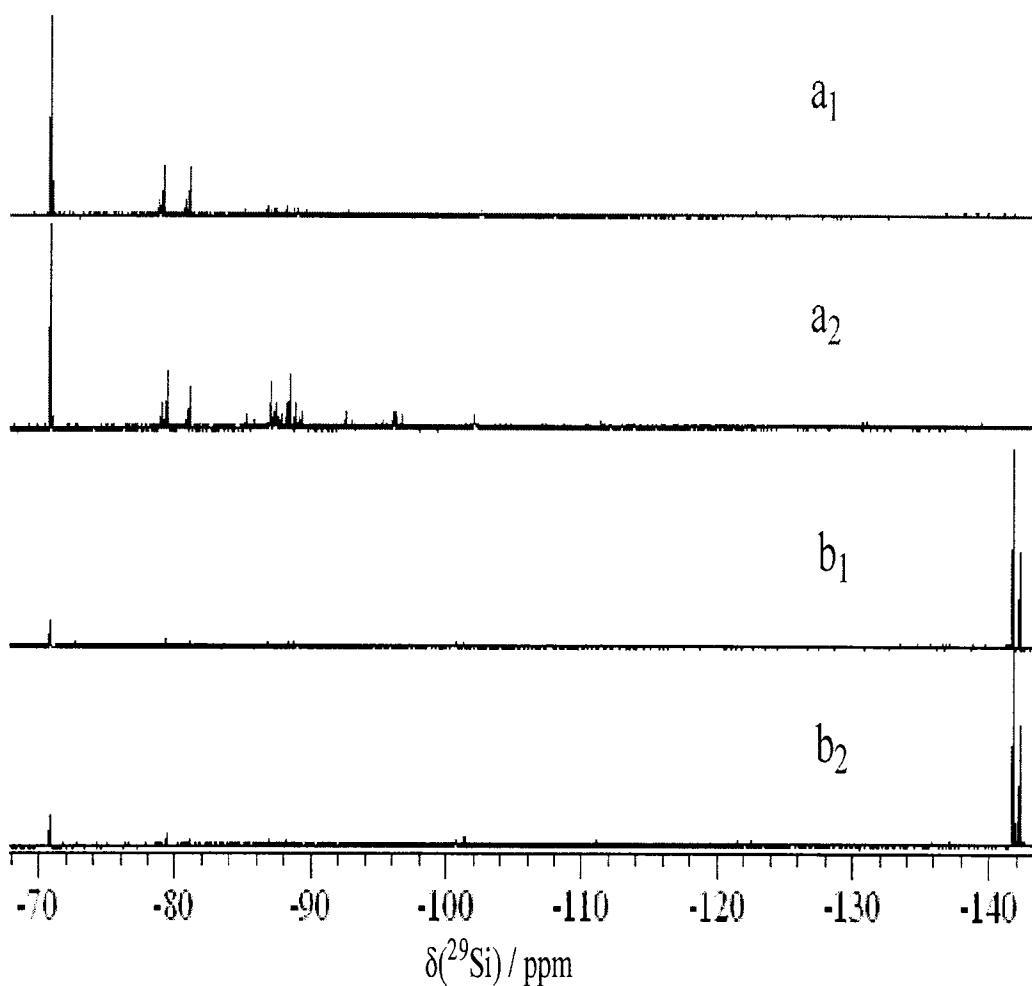
Figure 3.4.1. Silicon-29 NMR (99.36 MHz) spectra at 22 °C of solutions adjusted to

pH 12.30 ± 0.01 and containing: (a$_1$) 1.00 mol kg^{-1} SiO$_2$, 2.50 mol kg^{-1} D-arabitol and

3.06 mol kg^{-1} Na$^+$; (a$_2$) 0.99 mol kg^{-1} SiO$_2$, 2.48 mol kg^{-1} D-arabitol and 1.06 mol

kg^{-1} Na$^+$; (b$_1$) 0.89 mol kg^{-1} SiO$_2$, 2.23 mol kg^{-1} potassium D-gluconate and 2.67 mol

kg^{-1} Na$^+$; and (b$_2$) 1.02 mol kg^{-1} SiO$_2$, 2.32 mol kg^{-1} potassium D-gluconate and 1.02

mol kg^{-1} Na$^+$.

43
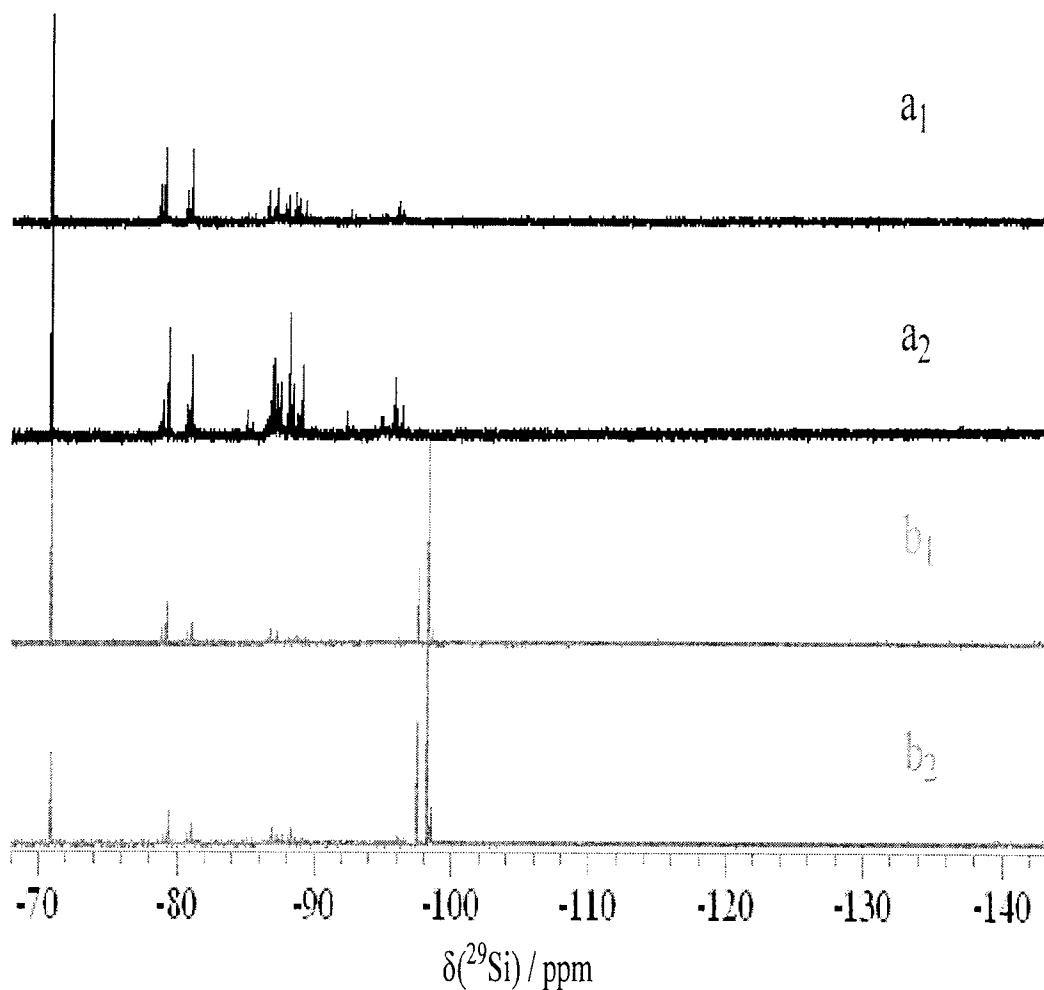
Figure 3.4.2. Silicon-29 NMR (99.36 MHz) spectra at 22 °C of solutions adjusted to

pH 12.30 ± 0.01 and containing: (a₁) 0.90 mol kg⁻¹ SiO₂, 2.30 mol kg⁻¹

1,2-cyclopentanediol and 2.71 mol kg⁻¹ Na⁺; (a₂) 0.98 mol kg⁻¹ SiO₂, 2.24 mol kg⁻¹

1,2-cyclopentanediol and 0.98 mol kg⁻¹ Na⁺; (b₁) 0.92 mol kg⁻¹ SiO₂, 2.36 mol kg⁻¹

anhydroerythritol and 2.75 mol kg⁻¹ Na⁺; and (b₂) 0.97 mol kg⁻¹ SiO₂, 2.22 mol kg⁻¹

anhydroerythritol and 0.97 mol kg⁻¹ Na⁺.
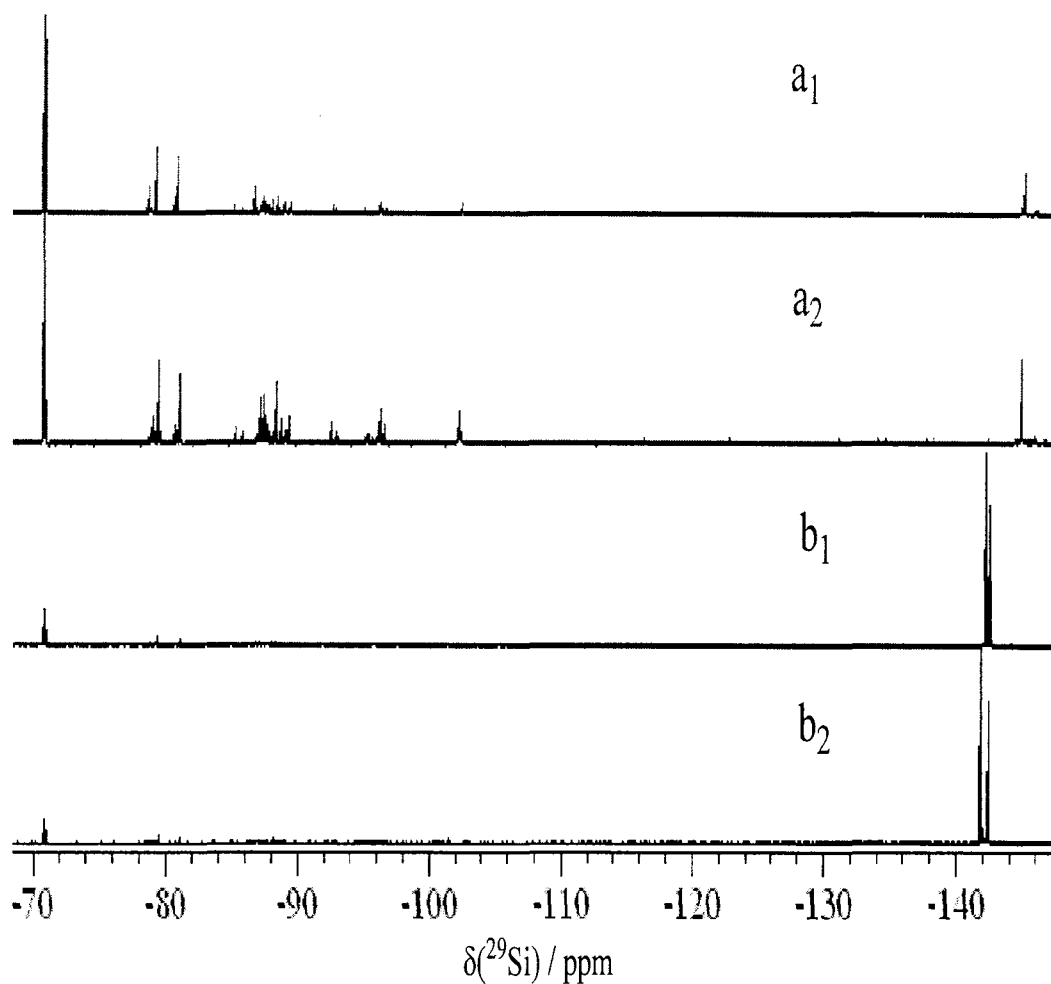
Figure 3.4.3. Silicon-29 NMR (99.36 MHz) spectra at 2 °C of solutions adjusted to

pH 12.30 ± 0.01 and containing: (a_1) 0.95 mol kg^{-1} SiO$_2$, 2.38 mol kg^{-1} D-arabitol and

3.00 mol kg^{-1} Na$^+$; (a_2) 0.95 mol kg^{-1} SiO$_2$, 2.37 mol kg^{-1} D-arabitol and 0.95 mol

kg^{-1} Na$^+$; (b_1) 0.87 mol kg^{-1} SiO$_2$, 2.18 mol kg^{-1} potassium D-gluconate and 3.00 mol

kg^{-1} Na$^+$; and (b_2) 0.91 mol kg^{-1} SiO$_2$, 2.35 mol kg^{-1} potassium D-gluconate and 1.00

mol kg^{-1} Na$^+$.

45
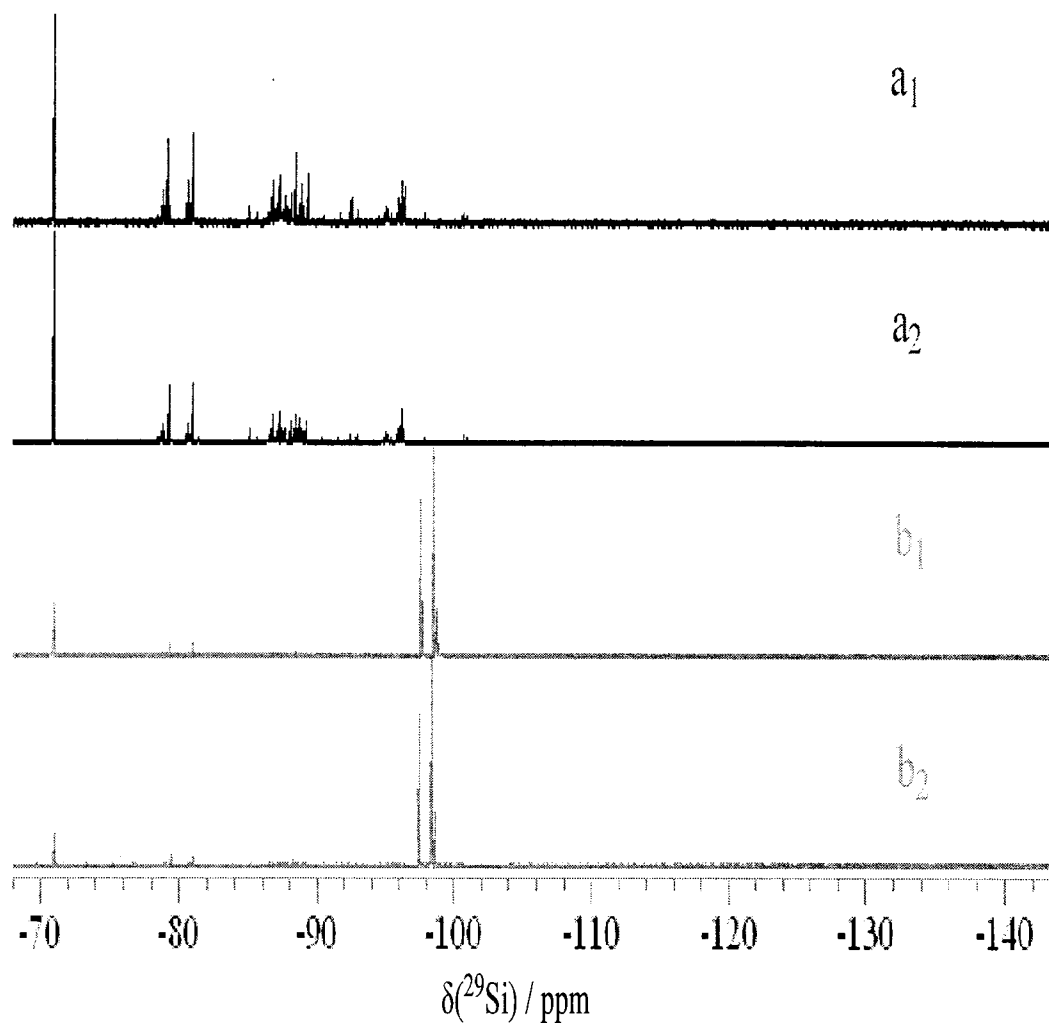
Figure 3.4.4. Silicon-29 NMR (99.36 MHz) spectra at 2 °C of solutions adjusted to

pH 12.30 ± 0.01 and containing: (a₁) 0.89 mol kg⁻¹ SiO₂, 2.28 mol kg⁻¹

1,2-cyclopentanediol and 2.99 mol kg⁻¹ Na⁺; (a₂) 0.91 mol kg⁻¹ SiO₂, 2.35 mol kg⁻¹

1,2-cyclopentanediol and 1.00 mol kg⁻¹ Na⁺; (b₁) 0.96 mol kg⁻¹ SiO₂, 2.66 mol kg⁻¹

anhydroerythritol and 3.00 mol kg⁻¹ Na⁺; and (b₂) 0.96 mol kg⁻¹ SiO₂, 2.45 mol kg⁻¹

anhydroerythritol and 1.00 mol kg⁻¹ Na⁺.
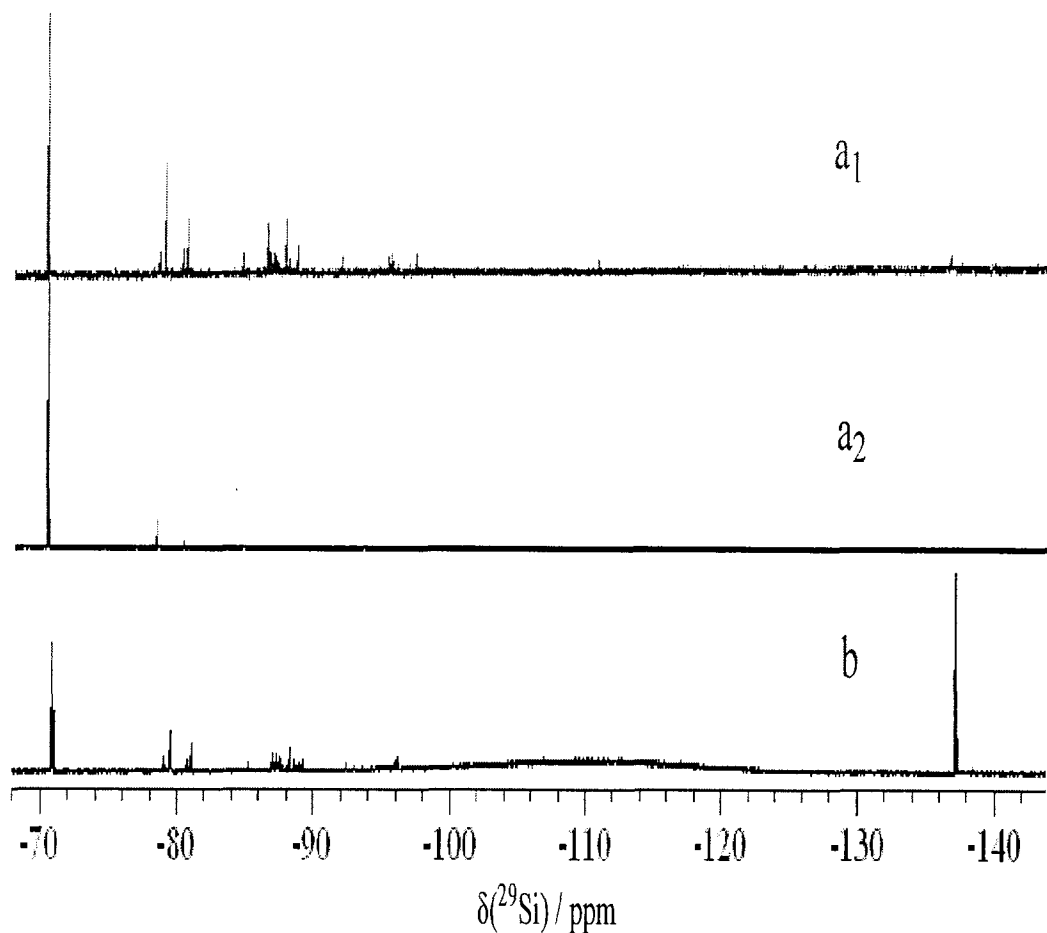
Figure 3.4.5. Silicon-29 NMR (99.36 MHz) spectra of solution adjusted pH 12.00 ±

0.01 containing: (a$_1$) 0.85 mol kg^{-1} SiO$_2$, 0.43 mol kg^{-1} guanosine and 1.82 mol kg^{-1}

Na$^+$ at 22 °C; (a$_2$) 0.85 mol kg^{-1} SiO$_2$, 0.43 mol kg^{-1} guanosine and 1.82 mol kg^{-1} Na$^+$

at 2 °C; and (b) 0.43 mol kg^{-1} SiO$_2$, 0.86 mol kg^{-1} guanosine and 1.72 mol kg^{-1} Na$^+$ at

–5 °C.

The formation of the pentaoxo- and hexaoxosilicon complexes can be

represented as follows. In this analysis, the three different diastereomers of [SiL$_2$]$^-$

are treated as a single entity as are the two diastereomers of [SiL$_3$]$^{2-}$.

47

• *Formation of the 5-coord Si complexes:*

$$H_3SiO_4^- + 2 \, L \rightleftharpoons [PL_2]^- + 3\,H_2O$$

or simply,

$$^1\underline{Q}^0 + 2\,L \rightleftharpoons [\underline{PL_2}]^- + 3\,H_2O$$
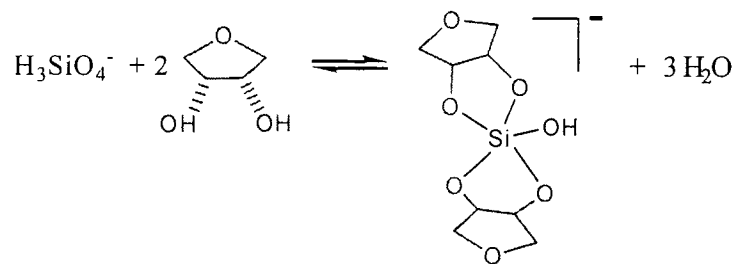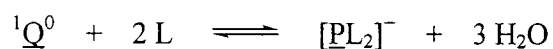
Using square parentheses to represent solute concentration, and assuming ideal solution behaviour, we obtain

$$K_{[\underline{PL2}]} = \frac{[\underline{PL_2}^-]}{[^1\underline{Q}^0]\,[L]^2}$$

• *Formation of the 6-coord Si complexes:*

or

$$^2\underline{Q}^0 + 3\,L \rightleftharpoons [\underline{HL_3}]^{2-} + 4\,H_2O$$
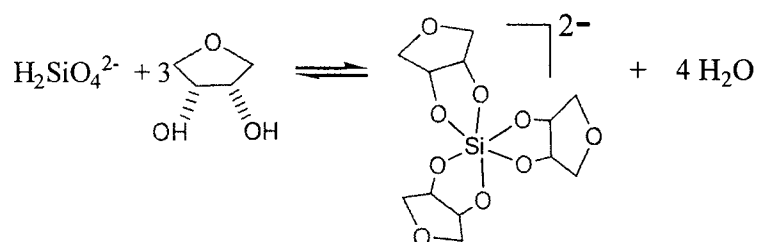
which yields

$$K_{[\underline{HL3}]} = \frac{[\underline{HL_3}^-]}{[^2\underline{Q}^0]\,[L]^3}$$

48

• *Silicic acid deprotonation equilibra* [66]:

$$H_4SiO_4 \rightleftharpoons H_3SiO_4^- + H^+$$

$$^0\underline{Q}^0 = {}^1\underline{Q}^0 + H^+ \qquad K_{a1} = 10^{-9.47}$$

and $\quad H_3SiO_4^- \rightleftharpoons H_2SiO_4^{2-} + H^+$
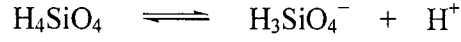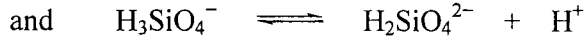
$$^1\underline{Q}^0 = {}^2\underline{Q}^0 + H^+ \qquad K_{a1} = 10^{-12.65}$$

The total silicate monomer concentration is given by:

$$[^T\underline{Q}^0] = [^0\underline{Q}^0] + [^1\underline{Q}^0] + [^2\underline{Q}^0]$$

Since $[^0\underline{Q}^0] \approx 0$ at pH 12,

$$[^T\underline{Q}^0] = [^1\underline{Q}^0] + \frac{[^1\underline{Q}^0]\, K_{a2}}{[H^+]}$$

$$[^1\underline{Q}^0] = \frac{[^T\underline{Q}^0]\, [H^+]}{K_{a2} + [H^+]}$$

and $\quad [^2\underline{Q}^0] = \dfrac{[^T\underline{Q}^0]\, K_{a2}}{K_{a2} + [H^+]}$

Therefore,

$$K_{[\underline{P}L2]} = \frac{[\underline{P}L_2^-]\,(K_{a2} + [H^+])}{[L]^2\,[^T\underline{Q}^0]\,[H^+]} \qquad\qquad [1]$$

and $\quad K_{[\underline{H}L3]} = \dfrac{[\underline{H}L_3^-]\,(K_{a2} + [H^+])}{[L]^3\,[^T\underline{Q}^0]\,[H^+]} \qquad\qquad [2]$

49

Accordingly, stability constants $K_{[PL2]}$ and $K_{[HL3]}$ were calculated from the

integrated spectra in Fig. 3.4.1 – 3.4.5. The results are presented in Tables 3.4.1 and

3.4.2. Following pH adjustment, the only significant difference between the two sets

of solutions prepared for each ligand and temperature was the NaCl concentration.

A close survey of the spectra in Fig. 3.4.1 – 3.4.5 shows that the silicate equilibria are

shifted in favour of the hexaoxosilicon complexes in the solutions with elevated salt

concentration. Therefore, only the solution set with [Na]:[Si] = 1.0:1 were used to

calculate stability constants $K_{[PL2]}$ and $K_{[HL3]}$. The overall findings are summarized

in Table 3.4.3.

Table 3.4.1. Stability constants of silicate complexes at 22 °C, pH = 12.30 ± 0.01,

and [Na]:[Si] = 1.0:1.

Ligand	Solute concentration (mol kg^{-1})			$K_{[PL2]}$	$K_{[HL3]}$
	SiO$_2$	Ligand	Na$^+$		
D-arabitol	0.99	2.48	1.06	0.207	4.89×10^{-2}
D-gluconic acid	1.02	2.32	1.02	10.8	175
cis-1,2-cyclo-pentanediol	0.98	2.24	0.98	0.109	a
1,4-anhydro-erythritol	0.97	2.22	0.97	6.96	a
guanosine ^{b}	0.43	0.85	1.82	1.28	13.0

^{a} Complex concentration is too small to enable calculation of the stability constant.

^{b} pH = 12.00 for this solution.

Table 3.4.2. Stability constants of silicate complexes at 2 °C, pH = 12.20 ± 0.01, and [Na]:[Si] = 1.0:1.

Ligand	Solute concentration (mol kg^{-1})			$K_{[PL2]}$	$K_{[HL3]}$
	SiO$_2$	Ligand	Na$^+$		
D-arabitol	0.95	2.37	1.00	0.190	0.664
D-gluconic acid	0.94	2.36	1.00	576	3.74×10^5
cis-1,2-cyclo-pentanediol	0.91	2.35	1.00	0.0377	a
1,4-anhydro-erythritol	0.96	2.45	1.00	21.4	a
guanosine b	0.43 c	0.86	1.72	a	559

a Complex concentration is too small to enable calculation of the stability constant.
b pH = 12.00 and at –5 °C for this solution.

Table 3.4.3. Summary of silicate complex stability constants.

Ligand	$K_{[PL2]}$		$K_{[HL3]}$	
	2 °C a	22 °C b	2 °C a	22 °C b
D-arabitol	0.190	0.207	0.664	4.89×10^{-2}
D-gluconic acid	576	10.8	3.74×10^5	175
cis-1,2-cyclo-pentanediol	0.0377	0.109	c	c
1,4-anhydro-erythritol	21.4	6.96	c	c
guanosine	c	1.28	559 d	13.0 e

a pH = 12.20 ± 0.01. b pH = 12.30 ± 0.01. c Complex concentration is too small to enable calculation of the stability constant. d pH = 12.00 and at –5 °C for this solution. e pH = 12.00 for this solution.

51

Figure 3.4.6 shows the ^{11}B NMR spectra of various boron-carbohydrate

solutions at 24 °C. The signal at −17.6 ppm corresponds to the borate anion

B(OH)$_4^-$. Whereas silicon exclusively binds acyclic polyols at their *threo*-pairs of

hydroxy groups, boron forms diester linkages at both *threo* and *erythro* hydroxy group

pairs [61, 67-72]. In Fig 3.4.6 (b) and (c), for example, ^{11}B NMR peaks located

between −13.4 and −13.7 ppm and at *ca.* −9.5 ppm correspond, respectively, to

mono-ligand ([B⁻L]) and *bis*-ligand ([B⁻L$_2$]) complexes in which boron is bound only

at *threo* hydroxy sites [70-72]. The signals at *ca.* −18 ppm correspond to

mono-ligand complexes in which boron is coordinated at *erythro* sites [71].

Additionally, peaks located between −13.8 and −14.8 ppm represent *mono*-ligand

diboron ([B⁻$_2$L]) complexes. In the case of furanoidic-*cis*-1,2-diol ligands, boron is

again able to form both *mono*- and *bis*-ligand complexes. The corresponding ^{11}B

NMR peaks are located at −12.5 to −13.4 ppm and −7.8 to −9.0 ppm, respectively, as

shown in Fig 3.4.6 (d)-(f) [72].

The equilibrium between boric acid B^0 and the borate ion B$^-$ is given by:

$$B(OH)_3 + OH^- \rightleftharpoons B(OH)_4^-$$

or $$B^0 + OH^- \rightleftharpoons B^-$$
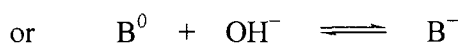
$$K_a = \frac{[B^-]}{[B^0][OH^-]} = 4.0 \times 10^4 \quad [70].$$

At pH 12.0, therefore, the concentration of B(OH)$_3$ in solution is negligible. The

formation of the *mono*-ligand boron complex (B⁻L), *bis*-ligand boron complex (B⁻L$_2$)
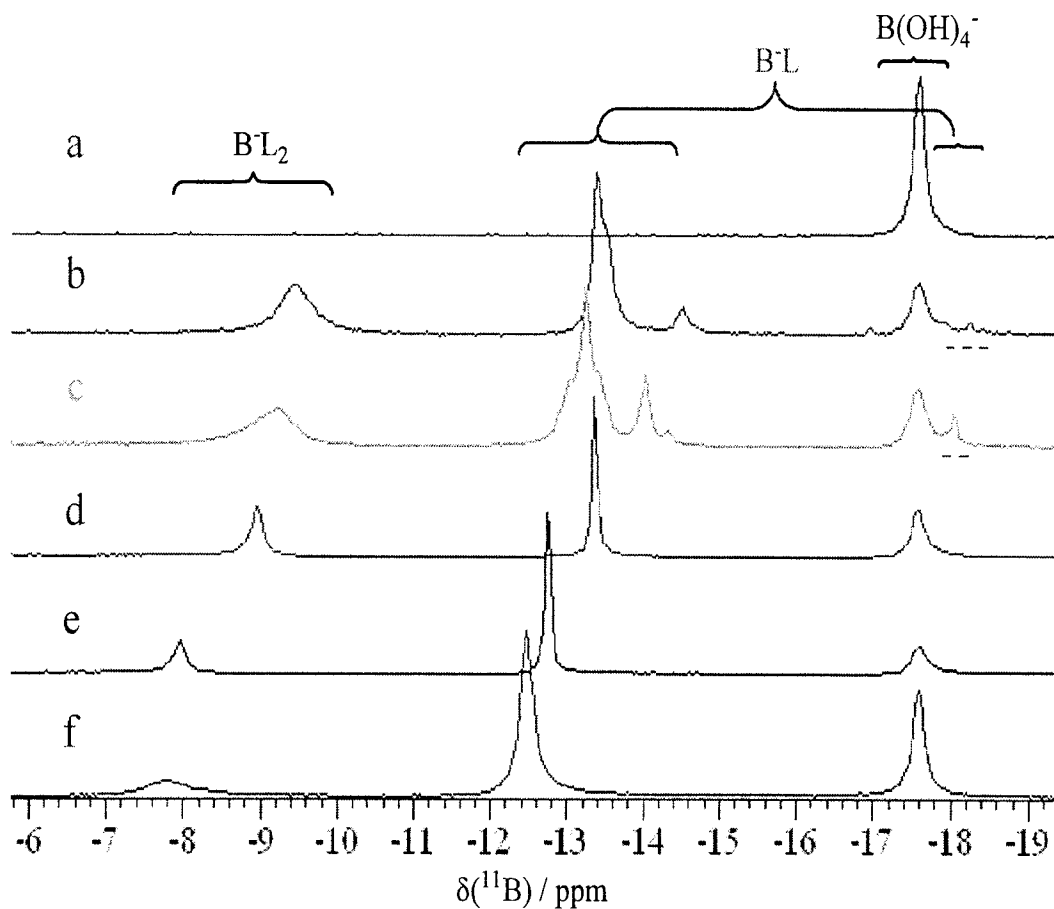
52

Figure 3.4.6. Boron-11 NMR (160.33 MHz) spectra at 24 °C corresponding to solutions that have been adjusted to pH 12.03 ± 0.03 and contain: (a) 0.10 mol kg^{-1} H_3BO_3; (b) 0.11 mol kg^{-1} H_3BO_3 and 0.11 mol kg^{-1} D-arabitol; (c) 0.10 mol kg^{-1} H_3BO_3 and 0.10 mol kg^{-1} potassium D-gluconate; (d) 0.11 mol kg^{-1} H_3BO_3 and 0.11 mol kg^{-1} cis-1,2-cyclopentanediol; (e) 0.10 mol kg^{-1} H_3BO_3 and 0.10 mol kg^{-1} 1,4-anhydroerythritol; and (f) 0.11 mol kg^{-1} H_3BO_3 and 0.11 mol kg^{-1} guanosine.

53

and *mono*-ligand diboron complex (B^-_2L) can be represented as follows [61, 70-72].

- $B^- + L \rightleftharpoons B^-L + 2\,H_2O$

$$K_{[B\text{-}L]} = \frac{[B^-L]}{[B^-][L]}$$

- $B^-L + L \rightleftharpoons B^-L_2 + 2\,H_2O$

$$K_{[B\text{-}L2]} = \frac{[B^-L_2]}{[B^-L][L]}$$

or $\quad B^- + 2\,L \rightleftharpoons B^-L_2 + 4\,H_2O$
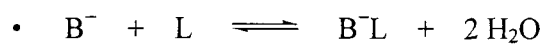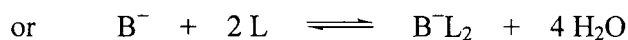
$$K'_{[B\text{-}L2]} = \frac{[B^-L_2]}{[B^-][L]^2}$$

where $\quad K'_{[B\text{-}L2]} = K_{[B\text{-}L]} \times K_{[B\text{-}L2]}$

- $B^- + B^-L \rightleftharpoons B^-_2L + 2\,H_2O$

$$K_{[B\text{-}2L]} = \frac{[B^-_2L]}{[B^-][B^-L]}$$

or $\quad 2\,B^- + L \rightleftharpoons B^-_2L + 4\,H_2O$
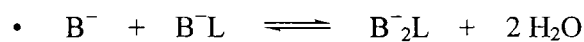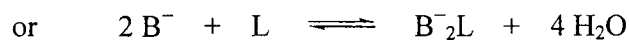
$$K'_{[B\text{-}2L]} = \frac{[B^-_2L]}{[B^-]^2[L]}$$

$$K'_{[B\text{-}2L]} = K_{[B\text{-}L]} \times K_{[B\text{-}2L]}$$

54

The total ligand concentration in solution from all sources is given by

$$C_L = [L] + [B^-L] + 2[B^-L_2] + [B^-_2L]$$

Thus,

$$[L] = C_L - [B^-L] - 2[B^-L_2] - [B^-_2L]$$

and

$$K_{[B-L]} = \frac{[B^-L]}{[B^-](C_L - [B^-L] - 2[B^-L_2] - [B^-_2L])} \qquad [3]$$

$$K_{[B-L2]} = \frac{[B^-L_2]}{[B^-L](C_L - [B^-L] - 2[B^-L_2] - [B^-_2L])} \qquad [4]$$

$$K'_{[B-L2]} = \frac{[B^-L_2]}{[B^-](C_L - [B^-L] - 2[B^-L_2] - [B^-_2L])^2} \qquad [5]$$

Stability constants $K_{[B-L]}$, $K_{[B-L2]}$ and $K'_{[B-L2]}$ were calculated for alkaline solutions at 24 °C from the integrated spectra in Fig. 3.4.6. (Since the diboron complex was a negligible component of these solutions, it was not considered in the present analysis.) The calculated stability constants are given in Table 3.4.4, and compared with those we obtained for the corresponding Si-complexes in Table 3.4.5. In addition, Tables 3.4.6 and 3.4.7 show values reported in the literature for B-complexes formed in alkaline solution (pH 11-12) at 25 °C with various dihydroxy [70] and acyclic polyol ligands [71]. Data reported for furanoidic cis-diol boron complexes formed in neutral solution at 25 °C [72] are listed in Table 3.4.8.

55

Table 3.4.4. Boron-11 NMR chemical shifts and stability constants of boron complexes formed with acyclic polyol and furanoidic cis-1,2-diol ligands in alkaline solution at 24 °C. [a]

Ligand (binding sites)		δ/ppm BL⁻	δ/ppm B⁻L₂	$K_{[B^-L]}$		$K_{[B^-L2]}$	$K'_{[B^-L2]}$
	(threo)	−13.6	−9.60	28.9			
D-arabitol	(erythro-3,4)	−14.2		4.02	35.4	5.64	200
	(erythro-1,3)	−18.1		2.50			
	(threo)	−13.2	−9.25	37.5			
gluconic acid	(erythro-4,5)	−14.0		11.8	66.2	3.16	209
	(erythro-2,4)	−18.2		16.9			
cis-1,2-cyclopentanediol		−13.4	−9.3	10.9		6.20	67.9
1,4-anhydroerythritol		−12.8	−12.8	22.2		4.15	92.1
guanosine		−12.4	−12.4	16.6		2.75	45.6

[a] In solutions containing 0.1 mol kg⁻¹ boric acid and 0.1 mol kg⁻¹ ligand at pH 12.0.

Table 3.4.5. Stability constants of silicon and boron complexes

Ligand	Si complexes at 22°C		B complexes at 24°C		
	$K_{[PL2]}$	$K_{[HL3]}$	$K_{[B^-L]}$	$K_{[B^-L2]}$	$K'_{[B^-L2]}$
D-arabitol	0.207	4.89×10^{-2}	35.4	5.63	200
gluconic acid	10.8	1.75×10^{2}	66.2	3.16	209
cis-1,2-cyclopentanediol	0.109	a	10.9	6.20	67.9
1,4-anhydroerythritol	6.96	a	22.2	4.15	92.1
guanosine	1.28	13.0	16.6	2.75	45.6

Table 3.4.6. Literature data for ^{11}B NMR chemical shifts and stability constants of boron complexes formed with dihydroxy ligands in alkaline solution at 25 °C [70].[a]

Ligand	δ / ppm		$K_{[B^-L]}$	$K_{[B^-L2]}$	$K'_{[B^-L2]}$
	B^-L^-	B^-L_2			
1,2-ethanediol	-13.7	-10.0	1.0	-	
1,2-propanediol	-13.6	-9.9	1.4	0.4	0.56
(±)-2,3-butanediol	-13.6	-9.6	8.7	2.4	20.9
cis-1,2-cyclopentanediol	-13.6	-9.4	33.3	78.1	2600
cis-1,2-cyclohexanediol	-14.2	-10.7	1.2	-	
trans-1,2-cyclohexanediol	-14.3	-	<0.1	-	
1,3-propanediol	-18.4	-19.8	0.9	-	
1,3-butanediol	-18.2	-18.9	1.9	-	

[a] Solutions contain 0.1 mol l^{-1} boric acid and 0.1 mol l^{-1} ligand at pH 12.

Table 3.4.7. Literature values for ^{11}B NMR chemical shifts and stability constants of boron complexes formed with acyclic polyols in alkaline solution at 25 °C [71]. [a]

| Ligand (binding sites) | | δ / ppm | | $K_{[B^-L]}$ | $K_{[B^-L2]}$ | $K'_{[B^-L2]}$ |
		B^-L^-	B^-L_2			
	(*threo*-2,3)	−13.2	−9.3	44	13	572
arabinonate	(*erythro*-3,4)	−14.2		10		
	(4,5)	−13.5		18		
	(2,4/3,5)	−18.1		0.31		
	(*erythro*-2,3)	−13.8	−9.9	13	4.3	55.9
ribonate	(*erythro*-3,4)	−14.4		6.6		
	(4,5)	−13.3	−9.3	10	0.98	9.8
	(2,4)	−18.0		14		
	(*threo*)	−13.4	−9.4	240	31	7440
gluconate	(*erythro*-4,5)	−14.2		72		
	(2,4)	−18.2		19		
	(*threo*-3,4)	−13.4	−9.2	1200	48	57600
mannonate	(*erythro*-4,5)	−14.5		140		
	(2,4/3,5/4,6)	−18.3		54		

[a] Solutions contain 0 to 0.15 mol l^{-1} boric acid and 0 to 1 mol l^{-1} ligand, respectively. Measurements were performed with D_2O as solvent at pD = 11.0.

58

Table 3.4.8. Literature data for ^{11}B NMR chemical shifts and stability constants of boron complexes formed with furanose ligands in neutral solution at 25 °C [72].[a]

Ligand (binding sites)		δ / ppm		$K_{[B^-L]}$
		B^-L	B^-L_2	
β-arabinofuranose	(1/2)	−13.7	−9.2	6000
	(1/2/5)	−13.0		[b]
β-fructofuranose	(2/3)	−13.7		6000
	(2/3/6)	−13.0		[b]
α-glucofuranose	(1/2)	−13.0	−8.5	45000
	(1/2 + 5/6)			[b]
	(1/2 + 3/5)			[b]
	(1/2 + 3/5/6)			[b]

[a] Solutions contain 0.1 mol l^{-1} boric acid and 0.1 mol l^{-1} ligand at pH 7.

[b] The stability constants of these esters could not be determined because of the low amount of free carbohydrate ligand present under the conditions in which these esters occurred.

59

Unlike the three furanoidic *cis*-diol ligands (*cis*-1,2-cyclopentanediol,

1,4-anhydroerythritol and guanosine) with only one binding site (*threo*), there are

three different binding sites in the two acyclic polyol ligands, D-arabitol with *threo*,

erythro-3,4 and *erythro*-1,3 binding sites and gluconic acid with *threo*, *erythro*-4,5 and

erythro-2,4 binding sites.   As shown in Table 3.4.4, the binding affinity of the *threo*

sites is larger than that of the *erythro* binding sites. Among the five investigated

ligands, the two acyclic polyol ligands gluconic acid and D-arabitol show larger

binding affinity ($K'_{[B-L2]}$ = 209 and 200, respectively) than the three furanoidic

cis-diol ligands which decreases in the order of 1,4-anhydroerythritol ($K'_{[B-L2]}$ = 92) >

cis-1,2-cyclopentanediol ($K'_{[B-L2]}$ = 68) > guanosine ($K'_{[B-L2]}$ = 46). The $K'_{[B-L2]}$

value of B-complex formed with gluconic acid is 3 times larger than that of

B-complex formed with cyclopentane diol, which is consistent with the literature data

reported by van Bekkum and co-workers [70-72].

Further comparison of the stability constants of silicate complexes with those

of borate complexes shows that: (i) the stability constant of the two acyclic polyol

ligands, $K'_{[B-L2]}$ = 205 ± 10 at 24 °C, the stability constant of the three furanoidic

cis-diol ligands, $K'_{[B-L2]}$ = 69 ± 23 at 24 °C, these values are, on average, roughly

100 times greater than those obtained for the analogous *bis*-ligand silicon complexes

($K_{[PL2]}$); and (ii) gluconic acid, cyclopentanediol and guanosine yield approximately

comparable stability constants for $\underline{P}L_2^-$ (10.8, 7.0 and 1.3) and B^-L_2 (3.2, 4.2 and 2.8,

respectively), indicating that silicon may play a similar mechanistic role as boron in

biological systems.

Conclusions

In the present study, we have employed ^{29}Si and ^{13}C NMR spectroscopy to determine the structures of organosilicate species in alkaline aqueous solution, namely pentaoxosilicon complexes formed with acyclic polyol ligands and hexaoxosilicon complexes formed with both acyclic polyol and furanoidic *cis*-diol ligands. All species are proved to be monomeric.

The five-coordinate Si complexes formed with acyclic polyols are structurally analogous to the monomeric [(L=)$_2$SiOH]$^-$ species obtained with furanoidic *cis*-diol ligands, each containing a single silicon centre bound via ester linkages to two bidentate ligands. However, they tend to be much shorter lived, presumably owing to the greater steric interaction existing between polyol ligands. Some of the pentaoxosilicon complexes formed with glucoheptonic acid are exceptions to this rule. This particular polyol is able to wrap around the pentaoxosilicon centre with all of its hydroxy groups directed inwards, resulting in three unique long-lived mono-ligand complexes – with two ([L=Si(OH)$_3$]$^-$), three ([L≡Si(OH)$_2$]$^-$) or four ([L≡SiOH]$^-$) ester linkages – and the usual array of labile bis-ligand complexes ([(L=)$_2$SiOH]$^-$).

Two distinct hexaoxosilicon *tris*-ligand structures occur at elevated pH in solutions containing either acyclic polyol or furanoidic *cis*-diol ligands. Additional species appear if the ligand contains more than one bidentate binding site. We have determined that they are inequivalent diastereomers of [(L=)$_3$Si]$^{-2}$ with δ-δ-δ and δ-δ-λ ligand configurations. If the ligands are extremely bulky, as in the case of ribonucleosides such as adenosine and guanosine, the δ-δ-λ diastereomer is virtually

61

eliminated because of steric ligand interactions. It was therefore surprising to discover that solutions containing particular combinations of different ribonucleosides (*i.e.*, adenosine and guanosine, adenosine and uridine, guanosine and cytidine), contain both the δ-δ-δ and δ-δ-λ diastereomers. The latter configuration brings the two different ribonucleoside base groups face to face, inferring that the δ-δ-λ diastereomer is stabilized by multi-point H-bonding or π-stacking interactions between the bases.

Binding affinity constants were measured and compared for silicon and boron complexes of two representative acyclic polyol ligands, D-arabitol and D-gluconic acid, and three furanoidic *cis*-diol ligands, *cis*-1,2-cyclopentanediol, 1,4-anhydroerythritol and guanosine. The stability constant of the boron *bis*-ligand complex does not vary significantly for the different ligands. In the case of the two acyclic polyol ligands, the stability constant of $K'_{[B-L2]}$ = 205 ± 10 at 24 °C. For the three furanoidic *cis*-diol ligands, $K'_{[B-L2]}$ = 69 ± 23 at 24 °C. These values are, on average, roughly 100 times greater than those obtained for the analogous *bis*-ligand silicon complexes ($K_{[PL2]}$). Nevertheless, gluconic acid and guanosine show quite high binding affinity with silicon, yielding both bis-ligand pentaoxosilicon complexes ($K_{[PL2]}$ = 10.8 and 1.3, respectively) and tris-ligand hexaoxosilicon complexes ($K_{[HL3]}$ = 175 and 13, respectively). These results indicate that silicon may play a similar mechanistic role as boron in biological systems.

References

1. Liang Y., Hua H., Zhu Y., Zhang J., Cheng C., Romheld V. Importance of plant species and external silicon concentration to active silicon uptake and transport, *New Phytolog.*, 172 (2006) 63-72.

2. De La Rocha C., Passow U. Recovery of *thalassiosira weissflogii* from nitrogen- and silicon-starvation, *Limnol. Oceanogr.* 49 (2004) 245-255.

3. Carlisle E.M. The nutritional essentiality of silicon. *Nutr. Rev.*, 40 (1982) 193-198.

4. Carlisle E.M. Silicon as a trace nutrient, *Sci. Total Environ.*, 73 (1988) 95-106.

5. Nielsen F.H. Nutritional requirements for boron, silicon, vanadium, nickel, and arsenic: current knowledge and speculation, *FASEB*, 5 (1991) 2661-2667.

6. Knight C.T.G. Are zeolite secondary building units really red herrings? *Zeolites*, 10 (1990) 140-144.

7. Cundy C.S. The hydrothermal synthesis of zeolites: History and development from the earliest days to the present time, *Chem. Rev.*, 103 (2003) 663-702.

8. Allan J.M., Francois M.M.M. A proton buffering role for silica in diatoms, *Science*, 297 (2002) 1848-1850.

9. Skowronska-Ptasinska M.D., Vorstenbosch M.L.W., Van Santen R.A., Abbenhuis H.C.L Tianium silsesquioxanes grafted on three-dimensionally netted polysiloxanes: Catalytic ensembles for epoxidation of alkenes with aqueous hydrogen peroxide, *Angw. Chem. Int. Ed. Eg.*, 41 (2002) 637-639.

10. Desouky M., Jugdaohsingh R., McCrohan C.R., White K.N., Powell J.J. Aluminum-dependent regulation of intracellular silicon in the aquatic, *Appl. Biol. Sci.*, 99 (2002) 3394-3399.

11. Fauteux F., Rémus-Borel W., Menzies J.G., Bélanger R.R. Silicon and plant disease resistance against pathogenic fungi, *FEMS Microbiol. Lett.*, 249 (2005) 1-6.

12. Ma, J. F. Role of silicon in enhancing the resistance of plants to biotic and abiotic stresses, *Soil Sci. Plant Nutr.*, 50 (2004) 11–18.

13. Heine G., Tikum G., Horst W.J. Silicon nutrition of tomato and bitter gourd with special emphasis on silicon distribution in root fractions, *J. Plant Nutr. Soil Sci.*, 168 (2005) 600-606.

14. Eneji E., Inanaga S., Muranaka S., Li J., Hatton T., Tsuji W. Effect of calcium silicate on growth and dry matter yield of chloris gayana and sorghum sudanense under two soil water regimes, *Grass Forage Sci.*, 60 (2005) 393.

15. Rains D.W., Epstein E., Zasoski R.J. Aslam M. Active silicon uptake by wheat, *Plant Soil*, 280 (2006) 223-228.

16. Hodson M.J., White P.J., Mead A., Broadley M.R. Phylogenetic variation in the silicon composition of plants, *Ann. Bot.*, 96 (2005) 1027-1046.

17. Mitani N., Ma J.F., Iwashita T. Identification of the silicon form in xylem sap of rice, *Plant Cell Physiol.*, 46 (2005) 279-283.

18. Schwarz K. A bound form of silicon in glycosaminoglycans and polyuronides, *Proc. Nat. Acad. Sci.*, 70 (1973) 1608-1612.

19. Loeper J., Goy-Loeper J., Rozensztajn L., Fragny M. The antiatheromatous action of silicon, *Atherosclerosis*, 33 (1979) 397-408.

20. Carlisle E.M. Silicon: A requirement in bone formation independent of vitamin D_1, *Calcif. Tissue Int.*, 34 (1980) 27-34.

21. Jugdaohsingh R., Tucker K.L., Qiao N., Cupples L.A., Kiel D.P., Powell J.J. Dietary silicon intake is positively associated with bone mineral density in men and premenopausal women of the Framingham Offspring cohort, *Bone Min. Res.*, 19 (2004) 297-307.

22. Carlisle E.M. Silicon: a possible factor in bone calcification, *Science*, 167 (1970) 179–280.

23. Carlisle E.M. Silicon: an essential element for the chick, *Science*, 178 (1972) 619–621.

24. Seaborn C.D., Nielsen F.H. Dietary silicon and arginine affect mineral element composition of rat femur and vertebra, *Biol. Trace Elem. Res.*, 89 (2002) 239-250.

25. Hott M., Pollak C.D., Modrowski D., Marie P.J. Short-term effects of organic

silicon on trabecular bone in mature ovariectomized rats, *Calcif. Tissue Int.*, 53 (1993) 174-179.

26. Schwarz K., Milne D.B. Growth-promoting effects of silicon in rats, *Nature*, 239 (1972) 333-334.

27. Rico H., Gallego-Lago J.L., Hernandez E.R. Effect of silicon supplement on osteopenia induced by ovariectomy in rats. *Calcif. Tissue Int.*, 66 (2000) 53-55.

28. Belles M., Sanchez D.J., Gomez M., Corbellam J., Domingo J.L. Silicon reduces aluminum accumulation in rats: Relevance to the aluminum hypothesis of Alzhermer disease, *Alzheimer Dis. Assoc. Disord.*, 12 (1998) 83-87.

29. Peluso M.R., Schneeman B.O. A food-grade silicon dioxide is gypocholesterolemic in the diet of cholesterol-fed rats, *J. Nutr.*, 124 (1994) 853-860.

30. Forrest H. N. Trace elements in human health and disease. *J. Trace Elem. Exp. Med.*, 13 (2000) 113-129.

31. McNaughton S.A., Bolton-Smith C., Mishra G.D., Jugdaohsingh R., Powell J.J. Dietary silicon intake in post-menopausal women, *Brit. Nutr.*, 94 (2005) 813-817.

32. Burton A.C., Cornhill J.F., Canham P.B. Protection from cancer by 'silica' in the water supply of U.S. cities, *J. Environ. Pathol. Toxicol.*, 4 (1980) 31-40.

33. Williams F.M.K., Cherkas L.F., Spector T.D., MacGregor A.J. The effect of moderate alcohol consumption on bone mineral density: A study of female twins, *Annals Rheum. Dis.*, 64 (2005) 309-310.

34. Sripanyakorn S., Jugdaohsingh R., Elliott H., Walker C., Mehta P., Shoukru S., Thompson R.P.H., Powell J.J. The silicon content of beer and its bioavailability in healthy volunteers, *Brit. J. Nutr.*, 91 (2004) 403-409.

35. Jugdaohsingh R., Anderson S.H.C., Tucker K.L., Elliott H., Kiel D.P., Thompson R.P.H., Powell J.J. Dietary silicon intake and absorption, *Am. J. Clin. Nutr.*, 75 (2002) 887-893.

36. Dyck K.V., Cauwenbergh R.V., Robberecht H., Deelstra H. Bioavailability of silicon from food and food supplements, *Fresenius J. Anal. Chem.*, 363 (1999) 541-544.

37. Tucker K.L., Chen H., Hannan M.T.L., Cupples A., Wilson P.W.F., Felson D., Kiel D.P. Bone mineral density and dietary patterns in older adults: The Framingham osteoporosis study, *Am. J. Clin. Nutr.*, 76 (2002) 245-252.

38. Ma J.F., Mitani N., Nagao S., Konishi S., Tamai K., Iwashita T., Yano M. Characterization of the silicon uptake system and molecular mapping of the silicon transporter gene in rice, *Plant Physiol.*, 136 (2004) 3284–3289.

39. Kinrade S.D., DelNin J.W., Schach A.S., Sloan T.A., Wilson K.L., Knight C.T.G. Stable five- and six-coordinated silicate anions in aqueous solution, *Science*, 285 (1999) 1542-1545.

40. Kinrade S.D., Maa K.J., Schach A.S., Sloan T.A., Knight C.T.G. Silicon-29 NMR evidence of alkoxy substituted aqueous silicate anions. *J. Chem. Soc., Dalton Trans.* (1999) 3149-3150.

41. Iler R.K. The Chemistry of Silica (1979) Wiley, New York.

42. Kinrade S.D., Donovan C.H., Schach A.S. Knight C.T.G. Two substituted cubic octameric silicate cages in aqueous solution, *J. Chem. Soc., Dalton Trans.*, (2002) 1250-1252.

43. Hamilton R. M.Sc. Thesis, Lakehead University (2001)

44. Wang J., Balec Epstein E., Jugdaohsingh R., Knight C.T.G., Powell J.J., Rains D.W., Taylor C., Kinrade S.D. Investigations of the molecular basis for silicon biofunctionality. *6th Keele Meeting on Aluminium*, Buçaco, Portugal, February 27, 2005.

45. Kinrade S.D., Pole D.L. Effect of alkali-metal cations on the chemistry of aqueous silicate solutions, *J. Am. Chem. Soc.*, (1992) 4558-4563.

46. Knight C.T.G., Kinrade S.D. Comment on "Identification of precursor species in the formation of MFI zeolite in the TPAOH-TEOS-H_2O system", *J. Phys. Chem. B* (2002) 3329-3332.

47. Kinrade S.D., Swaddle T.W. Silicon-29 NMR studies of aqueous silicate solutions. 2. Transverse [29]Si relaxation and the kinetics and mechanism of silicate polymerization, *Inorg. Chem.*, (1988) 4259-4264.

48. Kinrade S.D., Hamilton R.J., Schach A.S. Knight C.T.G. Aqueous hypervalent

silicon complexes with aliphatic sugar acids, *J. Chem. Soc., Dalton Trans.*, (2001) 961-963.

49. Kinrade S.D., Gillson A.-M. E., Knight C.T.G. Silicon-29 NMR evidence of a transient hexavalent silicon complex in the diatom Navicula pelliculosa, *J. Chem. Soc., Dalton Trans.*, (2002) 307-309.

50. Kinrade S.D., Schach A.S., Hamilton R.J., Knight C.T.G. Evidence of pentaoxo organosilicon complexes in dilute neutral aqueous silicate solutions, *J. Chem. Soc., Chem. Commun.*, (2001) 1564-1565.

51. Sahai N. Calculation of ^{29}Si NMR shifts of silicate complexes with carbohydrates, amino acid, and carboxylic acids: Potential role in biological silica utilization, *Geochim. Cosmochim. Acta*, 68 (2004) 227-237.

52. Kubicki J.D., Heaney J.D. Molecular orbital modeling of aqueous organosilicon complexes: Implications for silica biomineralization, *Geochim. Cosmochim. Acta*, 67 (2003) 4113-4121.

53. Benner K., Klufers P., Vogt M. Hydrogen-bonded sugar alcohol trimers as hexadentate silicon chelators in aqueous solution, *Angw. Chem. Int. Ed.*, 42 (2003) 1058-1062.

54. Kinrade S.D., Deguns Eric W., Gillson A.M E., Knight C.T.G. Complexes of pentaoxo and hexaoxo silicon with furanoidic vicinal *cis*-diols in aqueous solution, *J. Chem. Soc., Dalton Trans.*, (2003) 3713-3716.

55. Kinrade S.D., Balec R. J., Schach A.S.S., Wang J., Knight C.T.G. The structure of aqueous pentaoxo silicon complexes with *cis*-1,2-dihydroxycyclopentane and furanoidic vicinal *cis*-diols, *J. Chem. Soc., Dalton Trans.*, (2004) 3241-3243.

56. Lambert J.B., Lu G., Singer S.R., Kolb V.M. Silicate complexes of sugars in aqueous solution, *J. Am. Chem. Soc.*, 126 (2004) 9611-9625.

57. Mori Y., Suzuki A., Yoshino K., Kakihana H. Complex formation of p-boronophenylalanine with some monosaccharides, *Pigment Cell Res.*, (1989) 273-277.

58. Shinmori H., Takeuchi M., Shinkai S. Spectroscopic detection of diols and sugars by a colour change in boronic acid-appended spirobenzopyrans, *J. Chem. Soc.*,

Perkin Trans., (1995) 1-3.

59. Roy G.I., Laferriere A.L., Edwards J.O. A comparative study of polyol complexes of arsenite, borate, and tellurate ions, *J. Inorg. Nucl. Chem.*, 4 (1957) 106-114.

60. Oshima K., Toi H., Aoyama Y. Complexation of phenyboronic acid with alkyl glycopyranosides and related polyols as studied by ^{11}B NMR spectroscopy, *Carbohyd. Lett.*, 1 (1995) 223-230.

61. Henderson W.G., How M.J., Kennedy G.R., Mooney E.F. The interconversion of aqueous boron species and the interaction of borate with diols: A ^{11}B NMR study, *Carbohyd. Res.*, (1973) 1-12.

62. O'Neill M.A., Ishii T., Albersheim P., Darvill A.G. Rhamnogalacturonan-II: Structure and function of a borate cross-linked cell wall pectic polysaccharide, *Annu. Rev. Plant Biol.*, 55 (2004) 109-139.

63. Hu H., Penn S.G., Lebrilla C.B., Brown P.H. Isolation and characterization of soluble boron complexes in higher plants, *Plant Physiol*, 113 (1997) 649-655.

64. Semmelhack M.F., Campagna S.R., Hwa C., Federle M.J., Bassler B.L. Boron binding with the quorum sensing signal AI-2 and analogues, *Org. Lett.*, 6 (2004) 2635-2637.

65. Hunt C.D. Dietary boron: an overview of the evidence for its role in immune function, *J. Trace Elem Exp Med*, 16 (2003) 291-306.

66. Knight, C.T.G.; Kinrade, S.D. (2001) A primer on the aqueous chemistry of silicon, *Stud. Plant Sci.*, 8 (Silicon in Agriculture), 57-84.

67. Verchere J.F., Hlaibi M. Stability constants of borate complexes of oligosaccharides, *Polyhedron*, (1987) 1415-1420.

68. Dawber J.G., Green S.I.E. A polarimetric and [11]B and ^{13}C nuclear magnetic resonance study of the reaction of the tetrahydroxyborate ion with polyols and carbohydrates, *J. Chem. Soc., Faraday Trans.*, 84 (1988) 41-56.

69. Berg R., Peters J.A., Bekkum H. The structure and (local) stability constants of borate esters of mono- and di-saccharides as studied by ^{11}B and ^{13}C NMR spectroscopy, *Carbohyd. Res.*, (1994) 1-12.

70. Makkee M., Kieboon A.P.G., van Bekkum H., Studies on borate esters III: Borate

esters of D-mannitol, D-fructose and D-glucose in water, *Recl. Trav. Chim. Pays-Bas*, 104 (1985) 230-235.

71. van Duin M., Peters J.A., Kieboon A.P.G., van Bekkum H. Studies on borate esters II: Structure and stability of borate esters of polyhydroxycarboxylates and related polyole in aqueous alkaline media as studied by ^{11}B NMR, *Tetrahedron*, 41 (1985) 3411-3421.

72. ven der Berg R., Peters J.A., van Bekkum H. The structure and (local) stability constants of borate esters of mono- and di-saccharides as studied by ^{11}B and ^{13}C NMR spectroscopy, *Carbohyd. Res.*, 253 (1994) 1-12.